PERACIO RAFAEL BUENO FERREIRA

METABOLIC PROFILE, ULTRASTRUCTURE AND GENE EXPRESSION OF BRAZILIAN-GINSENG [Pfaffia glomerata (SPRENG.) PEDERSEN] UNDER PHOTOAUTOTROPHIC GROWTH AND INTERACTION WITH NEMATODES

Tese apresentada a Universidade Federal de Viçosa como parte das exigências do Programa de Pós-Graduação em Fisiologia Vegetal, para obtenção do título de Doctor Scientiae.

VIÇOSA
MINAS GERAIS – BRASIL
2017

Ficha catalográfica preparada pela Biblioteca Central da Universidade Federal de Viçosa - Câmpus Viçosa

T
F383m
2017

Ferreira, Peracio Rafael Bueno, 1988-
Metabolic profile, ultrastructure and gene expression of brazilian-ginseng [*Pfaffia glomerata* (Spreng.) Pedersen] under photoautotrophic growth and interaction with nematodes / Peracio Rafael Bueno Ferreira. – Viçosa, MG, 2017.
xii, 92f. : il. (algumas color.) ; 29 cm.

Inclui apêndice.
Orientador: Wagner Campos Otoni.
Tese (doutorado) - Universidade Federal de Viçosa.
Inclui bibliografia.

1. *Pfaffia glomerata* - Biossíntese. 2. Nematoide. 3. 20-Hidroxiecdisona. I. Universidade Federal de Viçosa. Departamento de Biologia Vegetal. Programa de Pós-graduação em Fisiologia Vegetal. II. Título.

CDD 22 ed. 583.53

PERACIO RAFAEL BUENO FERREIRA

METABOLIC PROFILE, ULTRASTRUCTURE AND GENE EXPRESSION OF BRAZILIAN-GINSENG [*Pfaffia glomerata* (SPRENG.) PEDERSEN] UNDER PHOTOAUTOTROPHIC GROWTH AND INTERACTION WITH NEMATODES

Tese apresentada à Universidade Federal de Viçosa, como parte das exigências do Programa de Pós-Graduação em Fisiologia Vegetal, para obtenção do título de *Doctor Scientiae*.

APROVADA: 18 de julho de 2017.

Diego Ismael Rocha

Humberto Josué de Oliveira Ramos

Diego Silva Batista

Camilo Elber Vital

Wagner Campos Otoni
(Orientador)

DEDICO

Ao precioso presente que Deus me concedeu: Maria

AGRADECIMENTOS

A Deus, Beleza tão antiga e tão nova, agradeço pelo cuidado, pela fonte de amor, pela força perseverante, agradeço por ter escutado a minhas orações e me retirado do meu esconderijo, colocando-me diante de mim mesmo. À minha linda Maezinha Maria pela ponderosa intercessão juntamente com Santa Rita de Cássia, rogando pelos impossíveis da minha vida

Ao Acampamento Maanaim, JOAM e MUR por me lembrar a todo instante que Deus ainda conta comigo

À Universidade Federal de Viçosa por toda a infraestrutura disponível para execução do trabalho e ao Conselho Nacional de Pesquisa e Desenvolvimento (CNPq), pela concessão de bolsas de estudos.

Ao Prof W. C. Otoni por todo apoio, amizade, orientação, paciência, por ter acreditado em mim, e incentivado meu potencial. Ao Laboratório de Cultura de Tecidos (LCT/Bioagro), seus funcionários (Elci e Lili) e estudantes em especial à Dra. A. C. F. da Cruz por ter me ensinado tudo o que hoje sei sobre a Pfaffia; Dr. Diego S. Batista e Sérgio Heitor pela amizade incondicional, ao Dr. Marcos V. M. Pinheiro, Dr. Elyabe M. Matos, Dra. Andréa D. Koehler, Dra. Lorena M. Vieira, Anyela M. Ríos Ríos e Kristhiano Chagas, pelo apoio e amizade. Agradeço à Profa. Lays A. Nery pelo companheirismo, amizade e ajuda de forma incomparável e também ao Prof. Diego I. Rocha pela ajuda nas análises de ultraestrutura.

Ao NuBiomol, em especial Dr. Camilo E. Vidal, Edvaldo Barros, Larissa T. Cyrino e Nívea M. Vieira, pelo apoio, confiança e ajuda nas análises de metabolômica e proteômica

Ao Prof. Cosme Damião Cruz, do Departamento de Biologia Geral (UFV) por todo apoio no caminho das análises estatísticas a serem seguidas.

À minha família, em especial pais, irmãos, sobrinhos, minha esposa Itainá pela presença fiel em minha vida, cuidado incondicional, por simplesmente ser o que é. Agradeço à minha filha Maria, que nesses últimos anos trouxe sentido majoritário ao

meu viver, perfumou meu caminho, mudou minha trilha sonora, abriu os meus olhos para a vida, e me deu forças para superar a mim mesmo. Amo você minha pequetuca!!!

A todos os meus amigos, difícil lembrar o nome de todos: Luana, Ruth, Mateus, Thais, Bia e Alberto, Uyra, Luysa de Fátima, Rodrigo, Anderson, Neil, Humberto, Inae Paulineli, e em especial a família que me adotou em Viçosa: Ivone, Zete, Gabriela e Mariana (in memorian) e ao meu saudoso amigo e para sempre intercessor Paulinho (in memorian). Agradeço, ainda, pela direção espiritual do Pe Afrânio, Pe Cassimiro e Pe Sérgio.

A todos que pela minha memória caduca, não coloquei o nome, mas que estão presentes em lugares especiais em meu coração. Agradeço.

BIOGRAFIA

PERACIO RAFAEL BUENO FERREIRA, filho de Maruzam Bueno Ferreira e Marlene Simões Gomes, nasceu em 29 de fevereiro de 1988 na cidade de Contagem, estado de Minas Gerais. Casou-se em Viçosa, MG, com Itainá Gonçalves Andrade Bueno e tiveram uma filha chamada Maria Andrade Peracio Bueno.

Graduou-se em Ciências Biológicas (Bacharelado) em dezembro de 2009 pela Universidade Estadual de Montes Claros. Obteve o título de mestre em Agroquímica Orgânica em 2012, pela Universidade Federal de Viçosa. Na mesma Universidade iniciou o doutorado em Fisiologia Vegetal em novembro de 2012, tendo defendido a tese em julho de 2017.

SUMMARY

ABSTRACT

FERREIRA, Peracio Rafael Bueno, D.Sc., Universidade Federal de Viçosa, July, 2017. **Metabolic profile, ultrastructure and gene expression of brazilian-ginseng [Pfaffia glomerata (Spreng.) Pedersen] under photoautotrophic growth and interaction with nematodes.** Adviser: Wagner Campos Otoni. Co-adviser: Adriano Nunes Nesi.

Pfaffia glomerata is a plant whose importance comes to the active constituent 20-hydroxiecdysone (20E), an important phytoecdisteroid. 20E is similar to insect molting hormones, however, it is still poorly understood how plants produce 20E. Here, the content of 20E in P. glomerata was assessed in plants grown under in vitro photoautotrophic conditions or challenged with the nematode Meloidogyne javanica, under greenhouse conditions. The aim of this work was understand the biosynthesis of 20E in two accessions of P. glomerata (Ac 22 and 43) by means of metabolomics, ultrastructure and expression of two 20E biosynthesis-related genes. We verified that photoautotrophy system was efficient to stimulate the production of 20E under CO_2 enrichment (1000 $\mu L\ L^{-1}$) combined with Florialite® as supporting material. Florialite® led to well-developed chloroplast strucuture and increasing of morphometric measures. Interestingly, the photoautotrophic system influenced on photosynthesis intermediates (amino acids, sugars, and TCA), stress-(aromatic amines and shikimate), osmotic adjustment-related compounds (hydroxyproline, aspartate and myo-inositol). Markedly, urea seems to be a biomarker for low photoautotrophic conditions. The nematodes reduced many central metabolites of Ac 43 (notably organic acids), and accumulated important amino acids for nematode nutrition (isoleucine and valine). Ac 22, by its turn, accumulated sugars that are stress indicators and closely involved on the maturation of the nematodes. Notwithstanding, the Halloween genes (Phantom and Spook), only reported in insects, were expressed in P. glomerata and were influenced by nematode interaction, increasing expression on Ac 43 infected by nematode and increasing content of 20E. Conversely, Phantom and Spook were downregulated in Ac 22 infected with nematodes. The infection of nematode causes damage-induced accumulation of 20E in accessions of Pfaffia glomerata and that accumulation was modulated by the phantom and spook genes and by differences on metabolome. We infered that metabolism of

Pfaffia glomerata accessions 22 and 43 is characterized by distinct metabolic signatures under photoautrophic system and with nematode interaction.

RESUMO

FERREIRA, Peracio Rafael Bueno, D.Sc., Universidade Federal de Viçosa, julho de 2017. **Perfil metabólico, ultraestrutura e expressão gênica de ginseng-brasileir [Pfaffia glomerata (Spreng.) Pedersen] sob crescimento fotoautotrófico e interação com nematoides.** Orientador**:** Wagner Campos Otoni. Coorientador: Adriano Nunes Nesi.

Pfaffia glomerata é uma planta cuja importância provém do princípio ativo 20-hidroxiecdisona (20E), um importante fitoecdiesteroide. 20E é similar aos hormônios de muda dos insetos, entretanto ainda é pouco claro como as plantas produzem 20E. Nesse trablho, o teor de 20E em P. glomerata foi avaliado em plantas crescido sobre condições fotoautotrófica in vitro ou desafiadas com o nematoide Meloidogyne javanica sob condições de casa de vegetação. O objetivo desse trabalho foi entender a biossíntese de 20E em dois acessos de P. glomerata (Ac 22 e 43) por meio da metabolômica, ultraestrutura e expressão de dois genes relacionados a biossíntese de 20E. Foi verificado que o sistema fotoautotrófico foi eficiente no estímulo da produção de 20E sobre enriquecimento de CO_2 (1000 µL L^{-1}) combinado com Florialite® como material de suporte. Florialite® permitiu um melhor desenvolvimento da estrutura do cloroplasto e aumentou medidas morfométricas. Curiosamente, o sistema fotoautotrófico influencioi nos intermediários da fotossíntese (aminoácidos, açucares e TCA), compostos relacionados ao estresse (aminas aromáticas e ácido chiquímico), ao ajustamento osmótico (hidroxiprolina, ácido aspártico e mio-inositol). Notavelmente, ureia parece ser um biomarcador para baixas condições fotoautotróficos. Os nematoides reduziram muito metabólitos centrais do Ac 43 (particularmente ácidos organicos) e acumulou importantes aminoácidos importantes para nutrição do nematoide (isoleucina e valina). Ac 22 por sua vez, acumulou açucares que são indicadores de estresse e intimamente relacionados à maturação dos nematoides. Não obstante, os Halloween genes (Phantom e Spook), somente reportado em insetos, foram expressos em P. glomerata e foram influenciados pela interação com nematoides, aumentando sua expressão no Ac 43 quando infectado pelo nematoide e aumentando o teor de 20E. Por outro lado, Phantom e Spook foram regulados abaixo no Acesso 22 infectado por nematoide. A infecção por nematoides causa acúmulo de 20E induzido por danos nos

acessos de Pfaffia glomerata e esse acúmulo, foi modulado pelos Phantom e Spook e pelas diferenças no metaboloma. Pode-se inferir que o metabolismo dos acessos 22 e 43 de Pfaffia glomerata é caracterizado por padrões metabólicos distintos sob sistema fotoautotrórico e na interação com nematoide. We infered that metabolism of Pfaffia glomerata accessions 22 and 43 were characterized by distinct metabolic signatures under photoautrophic system and with nematode interaction.

INTRODUCTION

Pfaffia glomerata (Spreng) Pedersen (Amaranthaceae) is found in South America, and Brazil is the most important collection center for species of this genus for medicinal, food and comesmetic industries (Corrêa Júnior et al. 2008). P.glomerata has a high economic value due to the similarity of phytochemical characteristics of Korean ginseng (Panax ginseng) (De-Paris et al. 2000) and due to the production of the 20-hydroxyecdysone (20E) (Festucci-Buselli et al. 2008) and saponins (Vardanega et al. 2017). Due its economic relevance, the propagation of P. glomerata plays an essential role in producing raw material for the pharmaceutical industry (Saldanha et al. 2013 and Vieira et al. 2002.

20E has agrochemical, biotechnological, medicinal and pharmaceutical uses, and may potentially be involved in biochemical and physiological processes in plants (Festucci-Buselli et al. 2008), it acts as defense mechanism to protect plants against phytophagous insects (Dinan et al. 2009) and is analogue to the insect molting hormone (Lafont et al. 1991). Although the presence of 20E and other ecdysteroids in plants was demonstrated more than 30 years ago, little has been related since about their biosynthetic pathway(s), and whether it operates in a sequence that is similar to or different from that in Arthropodes is not known (Reixach et al. 1999). It is known that ecdysteroids are synthetized from cholesterol, which, in turn, is synthesized from mevalonic acid (Lafont 1998). Plant enzymes catalyzing hydroxylation of cholesterol during biosynthesis of ecdysteroids require further study. It is known that cytochrome P450-dependent monooxygenases catalyze introduction of hydroxyl groups in ecdysones and that ‘Halloween’ genes modulate hydroxylation in insect ecdysteroids. In plants, for instance spinach, that an enzyme analogous to the insect enzyme (Alekseeva 2004).

The in vitro tissue culture is an important strategy used elsewhere in the understanding the biosynthetic pathways of several important bioactive compunds in plants (Wang et al. 2017). This tool has a great potential to be applied to unreveal 20E biosynthesis Pfaffia (Iarema et al. 2012). P.glomerata was usually cultivated in vitro in a mixotrophic / heterotrophic system, however, previous findings showed that photoautotrophic micropropagation is a very promising system for both in vitro

production of secondary metabolites from P. glomerata and mass propagation of the species (Saldanha et al. 2013): the plants displayed higher photosynthetic rates and produced more 20E in vitro when grown under photoautotrophic conditions (Iarema et al. 2012; Saldanha et al. 2012, 2013, 2014). In addition, Corrêa et al. (2015) previously surveyed other accessions from the in vitro germplasm bank and demonstrated that they had different in vitro photoautotrophic potentials and biomass accumulation. Because polyploidization may increase photosynthetic performance, it may also have positive effects on the photoautotrophic potential of the species (Correa et al. 2016).

Increased CO_2 concentrations associated to an adequate supporting material allowed to changes in plant physiology, including ultrastructural changes (Lucchesini et al. 2006), altered metabolic profile (Badr et al. 2011), accumulation of secondary metabolites (Yang et al. 2010) and increasing of 20E in P. glomerata (Saldanha et al. 2014). Another 20E inducing condition in P. glomerata is the interaction with nematodes of the genus Meloidogyne. The use of the split-root system was applied and increased accumulation of the content of the 20E (Cruz 2011)

In this context, the aim of this work was to evaluate a profile metabolic, ultrastructure changes and genes expression P. glomerata on byosinthesis of 20E grown on photoautotrophic conditions in vitro and Meloidogyne javanica interaction ex vitro.

REFERENCES

Alekseeva LI (2004) Ecdysone 20-Monooxygenase Activity of Cytochrome P450 in Ajuga reptans L. Plants and Cell Culture. **Appl Biochem Microbiol**, 40: 135–139.

Badr A, Angers P, Desjardins Y (2011) Metabolic profiling of photoautotrophic and photomixotrophic potato plantlets (Solanum tuberosum) provides new insights into acclimatization. **Plant Cell Tiss Organ Cult**, 107:13-24.

Corrêa JPO, Vital CE, Pinheir MVM, Batista DS, Azevedo JFL, Saldanha CW, Cruz ACF, DaMatta FM, Otoni WC (2015) In vitro photoautotrophic potential and ex vitro photosynthetic competence of Pfaffia glomerata (Spreng.) Pedersen accessions**. Plant Cell Tiss Organ Cult,** 121:289–300

Corrêa JPO, Vital CE, Pinheiro MVM, Batista DS, Saldanha CW, Cruz ACF, Notini MM, Freitas DMS, DaMatta FM, Otoni WC (2016) Induced polyploidization increases 20-hydroxyecdysone content, in vitro photoautotrophic growth, and ex vitro biomass accumulation in Pfaffia glomerata (Spreng.) Pedersen. **In Vitro Cell Dev Biol Plant,** 52:45–55.

Cruz ACF(2011) **Interações entre acessos de fáfia [Pfaffia glomerata (Spreng.) Pedersen] com nematoides (Meloidogyne incognita e M. javanica): aspectos fitoquímicos e estruturais**. Tese (Doutorado em Botânica). Universidade Federal de Viçosa.

De Paris F, Neves G, Salgueiro JB, Quevedo J, Izquierdo I, Rates SMK (2000) Psychopharmacological screening of Pfaffia glomerata Spreng. (Amarathanceae) in rodents. **Ethnopharmacology**, 73: 261-269.

Dinan L, Harmatha J, Volodin V, Lafont R (2009) Phytoecdysteroids: Diversity, Biosynthesis and Distribution. In: Smagghe G. (Ed.). **Ecdysone: Structures and Functions**, Springer. p.43.

Festucci-Buselli RA, Contim LAS, Barbosa LCA, Stuart JJ, Otoni WC (2008) Biosynthesis and potential functions of the ecdysteroid 20-hydroxyecdysone – a review. **Botany**, 86: 978-987.

Iarema L, Cruz ACF, Saldanha CW, Dias LLC, Fontes RV, Oliveira EJ, Otoni WC (2012) Photoautotrophic propagation of Brazilian ginseng [Pfaffia glomerata (Spreng.) Pedersen]. **Plant Cell Tiss Organ Cult**, 110:227-238.

Lafont R, Bouthier A, Wilson ID (1991) Phytoecdysteroids: structures, occurrence, biosynthesis and possible ecological significance. In **Insect Chemichal Ecology** (Hardy, I ed.) Academia Praha and SBP Academic publishers, Praha. pp.197-214.

Lafont R. (1998)Physiology of Plants. **Fiziologya Rastenii** (Moscow), 45(3):276-295.

Lucchesini M, Moteforti G, Mensuali-Sodi A, Serra G (2006) Leaf ultrastructure, photosynthetic rate and growth of myrtle plantlets under different in vitro culture conditions. **Biol Plant**, 50: 161-168.

Reixach N, René L, Camps F, Casas J (1999) Biotrasnformation of putative phytoecdysteroid biosynthetic precursors in tissue culture of Polypodium vulgare. **Eur J Biochem**, 266:608-615.

Saldanha CW, Otoni CG, Rocha DI, Cavatte PC, Detmann KSC, Tanaka FAO, Dias LLC, DaMatta FM, Otoni WC (2014) A CO_2-enriched atmosphere and supporting material impact the growth morphophysiology and ultrastructure of in vitro Brazilian – ginseng [Pfaffia glomerata (Spreng.) Pedersen] plantlets. **Plant Cell Tiss Organ Cult,** 118:87-99.

Saldanha CW, Otoni CG, Azevedo JLF, Dias LLC, Rêgo MM, Otoni WC (2012) A low-cost alternative membrane system that promotes growth in nodal cultures of Brazilian ginseng [Pfaffia glomerata (Spreng.) Pedersen]. **Plant Cell Tiss Org Cult**, 110:413-422.

Saldanha CW, Otoni CG, Notini MN, Kuki KN, Cruz ACF, Neto AR, Dias LLC, Otoni WC (2013) A CO_2-enriched atmosphere improves in vitro growth of Brazilian ginseng [Pfaffia glomerata (Spreng.) Pedersen]. **In Vitro Cell Dev Biol Plant**, 49:433-444.

Vardanega R, Santos DT, Meireles MAA (2017) Proposal for fractionating Brazilian ginseng extracts: process intensification approach. **J Food Eng**, 196:73-80.

Vieira RF, Silva SR, Alves RBN, Silva DB, Wetzel MMVS, Dias TAB, Udry MC, Martins RC (2002) Estrate´gias para conservação e manejo de recursos genéticos de plantas medicinais e aromáticas. **Resultados da 1a Reunião Técnica. Embrapa Recursos Genéticos e Biotecnologia, Brasília**: Ibama, CNPq, Brasil, 184p

Wang J, Li JL, Li J, Li JX, Liu SJ, Huang LQ, Gao WY (2017) Production of Active Compounds in Medicinal Plants: From Plant Tissue Culture to Biosynthesis. **Chin Herbal Med**, 9: 115-125.

Yang L, Zambrano Y, Hu CJ, Carmona ER, Bernal A, Perez A, Zayas CM, Li YR, Guerra A, Santana I, Arencibia AD (2010) Sugarcane metabolites produced in CO_2-rich temporary immersion bioreactors (TIBs) induce tomato (Solanum lycopersicum) resistance against bacterial wilt (Ralstonia solanacearum). **In Vitro Cell Dev Biol Plant**, 46: 558-568

CHAPTER 1

Metabolic profile and ultrastructure provide new insights in in vitro photoautotrophic growth of the brazilian-ginseng [Pfaffia glomerata (Spreng.) Pedersen]

ABSTRACT

Studies have revealed the successful in vitro propagation of Pfaffia glomerata under photoautotrophic conditions with CO_2 enrichment. For this purpose, an efficient supporting material with high percent porosity in place of agar is required. The aim of this study was to investigate the role of supporting material and CO_2 enrichment on the growth, morpho-anatomy and metabolic profile of two accessions (22 and 43) of in vitro-grown P.glomerata subject to photoautotrophy condition. Most growth parameters, such as height, number of nodes, stem diameter, leaf area, adaxial and abaxial leaf perimeter, adaxial and abaxial leaf thickness, mesophyll thickness, midrib area and height and vascular bundle perimeter were greater under 1000 µL L^{-1} CO_2, using Florialite® as supporting material than with agar on both CO_2 concentrations and both accessions. CO_2 enrichment and supporting material had great influence on chloroplast lammelation pattern and ecdysone content. We identified a set of 49 different metabolites in leaf tissue. Using a concentration of 1000 µL L^{-1} and Florialite® it was clear that influenced prominently on photosynthesis intermediaries (amino acids, sugars, intermediaries of TCA), stress- (aromatic amines and shikimate), osmotic adjustment-related compounds (hidroxyproline, aspartate and myo-inositol). Urea seems to be a biomarker of low photoautotrophic competence. The accession 22 to has less tolerance to stress than accession 43, as indicate by the polyamine content. These findings provides a better understanding of how the supporting material has influence on Pfaffia glomerata in vitro metabolism under development photoautotrophic system; how photoautotrophy optimization increases 20-hydroxyecdysone content on Pfaffia glomerata by changes on primary metabolism levels and triggers chloroplasts maturation and the distint metabolic mechanism of accession 22 and 43 of Pfaffia glomerata under photoautrophic system.

Keywords: metabolomics, tissue culture, photoautotrophic growth, supporting material

INTRODUCTION

In traditional in vitro cultivation methods propagated plants show peculiar characteristics, such as poorly developed shoots, less epicuticular and cuticular waxes, high water content, non-functional and small stomata, thin leaves with few trichomes and low photoautotrophic activity (Xiao et al. 2011). In this system, plants are supplied with exogenous carbohydrates sources to sustain growth and development because the CO_2 concentration inside culture containers is reduced, which markedly limits photosynthesis (Kozai 2010). In vitro photoautotrophy can be performed by excluding carbohydrates from the médium and increasing gas exchange and improving photosynthetic photon flux (Xiao et al. 2011). Plants cultivated in photoautotrophy system have their water potential increased rapidly and higher water content and water use efficiency. Elevated CO_2 enhances the acclimatization process, diminishing plant mortality through the attenuation of plant damage and allowing better adaptation of plants to the environmental conditions (Pérez-Jimenez et al. 2015). Martins et al. (2016) obtained higher growth rates of Billbergia zebrina grown in vitro on photoautotrophic system, and inferred that photoautotrophic conditions interfere positively on ex vitro growth when previously cultivated in this system.

Currently, studies have revealed the successful in vitro propagation of Pfaffia glomerata under heterotrophic, photomixotrophic and photoautotrophic conditions (Iarema et al. 2012); with gas permeable membrane that allows natural ventilation in culture vessels (Saldanha et al 2012) and with CO_2-enrichment atmosphere wiht forced ventilation (Saldanha et al. 2013). For this successful in vitro propagation it is necessary an efficient supporting material with high porosity like Florialite® (Nisshinbo Industries, Inc., Tokyo) that contains a mixture of vermiculite and cellulose fiber (Afreen-Zobayed et al. 1999). Florialite® has been satisfactorily used in in vitro propagation of Pfaffia glomerata (Saldanha et al. 2014).

Pfaffia glomerata (“fáfia,“brazilian ginseng”), a medicinal plant that naturally grows in Brazil (Pott and Pott 1994), has great economic importance due to the production of secondary metabolites such as β-ecdysone (20E) (Festucci-Buselli et al. 2008) and triterpene saponins (Mroczek 2015). Several properties have been associated

with genus Pfaffia, such as anabolic, analgesic, antiinflammatory, antimutagenic, aphrodisiac, sedative, muscle tonic, antiviral and antifungal properties (Neto et al. 2005; Fernandes et al. 2005; Festucci-Buselli et al. 2008; Mendes 2011, Mroczek 2015). Many patents related to pharmacological and nutritional properties of Pfaffia have been published (Shibuyaetal 2001; Bernard and Gautier 2005; Olalde 2008; Rangel 2008; Loizou 2009; Higuchi 2011). Because of its economic relevance, the propagation of P. glomerata plays an essential role in producing raw material for the pharmaceutical industry (Saldanha et al. 2013), and as well for lessening the serious problems from the overharvesting this species from the wild.

The photoautotrophic potential and ex vitro photosynthetic competence of Pfaffia glomerata was recently reported (i et al. 2015); however up to now there are no studies that examine the photosynthetic competence of P. glomerata grown in vitro and their metabolic changes. A metabolic approach is usefeul on comprehensive analysis of tissue cultured plantlets (Badr et al 2015) and CO_2 effect on plants (Misra and Chen 2015).

Metabolism primary of plants are affected by elevetad CO_2 that triggers increases in carbono assimilitation and water-use efficiency result from global changes in metabolismo, including increases in the leaf C/N ratio and proportion of non-structural carbohydrates Secondary metabolism compounds respond to elevetade CO_2 between gymnosperms and angisperms and the changes in this metabolism may affect growth, development and fitness (Misra and Chen 2015).

Thus, the aim of this work was to define a metabolic profile of two environmental CO_2 atmospheres, supporting material, morpho-anatomical changes and 20E production, that could provide physiological signatures for Pfaffia glomerata grown under photoautotrophic in vitro conditions.

MATERIALS AND METHODS

Plant material and growth conditions

Pfaffia glomerata apexes (1 cm) from Accession 22 and 43 were obtained from in vitro grown donor plants previously kept in photomixotrophic conditions in MS salts and vitamins (Murashige and Skoog 1962), 100 mg L^{-1} myo-inositol and 7 g L^{-1} agar (Merck®), culture medium sterilized by autoclaving at 121 ° C and 0,15 Mpa for 15 min, and the pH adjusted to 5.7 with NaOH 1M.

The apexes were cultivated in sugar-free culture medium in culture room at 25 ± 2 ° C, irradiance of 150 μmol m^{-2} s^{-1} and 16 h photoperiod. The culture medium consisted in MS salts and vitamins (Murashige and Skoog 1962), 100 mg L^{-1} myo-inositol and 7 g L^{-1} agar (Merck®)/ (100 g) Florialite®.

For a normal atmosphere and enriched CO_2, the culture flasks were placed into two 41 x 26 x 60-cm, 4-mm-thick acrylic boxes with forced ventilation: on with the atmospheric concentracion of CO_2 (360 μL L^{-1}) and the other with external input of CO_2 (1000 μL L^{-1}), as described by Saldanha et al. (2013). The CO_2 concentration was adjusted using an infrared gas analyzer (model S153 CO_2 Analyzer System Qubit, Kingston, Canada).

The experiment was conducted in a completely randomized design with 5 replicates, composed by two propylene Magenta® (Sigma Chemical Co., USA) boxes connected by couplers (Sigma Chemical Co., USA), with 750 mL capacity. Each vessel contained, 120 mL of culture medium and 3 shoot apexes (experimental unit). The gas exchanges were allowed through two 10 mm diameter orifices in the lids, which were covered with hydrophobic polytetrafluoroethylene with 0.45 μm porous size membranes (PTFE; MilliSeal® AVS-045 Air Vent, Tokyo, Japan).

The treatments were arranged in a factorial design (2x2x2) consisting by two environments (360 ± μL L^{-1} and 1000 ± μL L^{-1}) combined with two types of explant support material: agar Merck® (Merck Millipore Corp., Darmstadt, Germany) or Florialite® (mixture of vermiculite and cellulose, Nisshinbo Industries, Japan)- with two Pfaffia accessions (Acession 22 and Acession 43).

Growth evaluation

After 45 days of in vitro culture, the height, the number of nodes and stem diameter were measured.

Micromorphometry and ultrastructure

For anatomical studies fully expanded leaves from second node were fixed in glutaraldehyde solution (Karnovsky 1965 modified - 2.5% glutaraldehyde, 4% paraformaldehyde, 3% sucrose, $CaCl_2$ 5 µM in cacodylate buffer 0.1M pH 6.8) for 24 h, dehydrated in ethanol series and embedded in methacrylate (Historesin, Leica). Cross sections with 5 µm will be obtained with a rotary microtome automatic advance (RM 2255 - Leica) equipped with a glass knife.

Sections were stained with toluidine blue at pH 4.4 (O'Brien and McCully, 1981) for 10 min, slides were mounted with synthetic resin (Permount). The analysis and photographic documentation was carried out under a light microscope (Olympus AX - 70) connected to a microphotography system (Olympus U- Photo). For the analysis of the dimensions nine cuts in three repetitions, were randomly sampled to measure blade area, adaxial and abaxia perimeter and thickness, mesophyll thickness, midrib height and vascular bundle perimeter, using the software Image Pro Plus version 4.1 for Windows (Media Cybernetics, Silver Spring, MD, USA).

For ultrastructural analysis of leaf samples of Pfaffia vitroplants were fixed in Karnovsky's solution [glutaraldehyde (2.5 %) and paraformaldehyde (4%) in sodium cacodylate buffer (pH 7.2) plus calcium chloride 5 mM] (Karnovsky 1965).

Subsequently, they were subjected to post-fixation with osmium tetroxide 1% dehydrated in an increasing series of acetone, infiltrated and polymerized in epoxy resin Spurr low viscosity. The blocks were prepared for ultramicrotomy on a dresser (EM Trim, Leica Microsystems Inc. USA).

Sections with 70 nm thickness were obtained in an ultramicrotome (Leica UC6, Leica Microsystems Inc., USA) and counterstained with uranyl acetate and lead citrate (Reynolds 1963). Analyses were performed in transmission electron microscope at 80 kV, EM900 (Carl Zeiss AG, Oberkochen, Alemanha) coupled with digital camera on NAP / MEPA (ESALQ /USP).

20-hyrdroxyecdysone content

The content of 20-hyrdroxyecdysone (20E) in Pfaffia glomerata shoot in all treatments was determined using high-performance liquid chromatography (HPLC) following the methodology proposed by Kamada et al. (2009). The methanolic extracts were analyzed by HPLC Shimadzu (LC- 10AI model, Tokyo, Japan) equipped with a CBM -10A detector Bondesil C18 chromatographic column (4.6 mm x 5.0 µm x 250 mm), mobile phase was methanol: water (1:1) in an isocratic flow 0.7 mL min $^{-1}$. The sample injection volume was 20 µL analyzed and wavelength 245 nm.

Pfaffia glomerata leaf metabolite sample preparation for CG-MS

Plant material was prepared for metabolite analysis according to Lisec et al. (2006), with modifications. Briefly, leaves of the plantlets were collected at the middle of the light period, frozen in liquid nitrogen and stored at -80 ºC until sample preparation. A 10 mg sample lyophilized leaf tissue was ground to a fine powder with a mortar and pestle in the presence of liquid nitrogen and then extracted with 1.5 mL of extraction buffer water: metanol:chloroform (1:2.5:1) and ribitol (200 µg mL^{-1}). Metabolites were extracted from the sample by incubation for 30 min at 4 °C and 950 rpm and then the supernatant (1 mL) was collected. It was added to the supernatant 750 µL of water, and then was centrifuged for 15 min, at 4°C, at 12000 rpm. Aliquot of 50 µL was collected and subsequently dried in a speed-vacuum. The residue was derivatized for 120 min at 37 °C (in 40 µL of 20 mg mL^{-1} methoxyamine hydrochloride dissolved in pyridine), followed by a 30-min treatment at 37 °C with 70 µL of MSTFA [N-methyl-N-(trimethylsilyl) trifluoroacetamide]. Prior to trimethylsilylation, 20µL of a retention time standard mixture was added - 3.7% (w/v) for hepatonic acid, nonanoic acid, undecanoic acid, and tridecanoic acid; 7.4% (w/v) for pentadecanic acid, nonadeanoic acid, and tricosanoic acid; 22.2% (w/v) for heptacosanoic acid; 55.5% (w/v) forhentriacontanoic acid dissolved in 10 mg/ mL^{-1} tetrahydrofuran. One-microliter volumes of sample were injected with a split ratio of 25:1.

GC-MS analysis

The separation was performing using na Agilent 7890 A GC equipped with a 30-m MDN-35 column (Macherey-Nagel) and analytes were detected using a LecoTruTOF® HT TOFMS (Leco Corporation, St Joseph, USA; Lisex et al. 2006). Samples (1µL) were injected in splitless mode at 230ºC usign helium as carrier gas as contínuos flow of 2 ml min^{-1}. The GC oven temperature was initially maitained constant as 80ºC and the increased at a rate of 15ºC min^{-1} to 330ºC. The chromatograms were aligned using the MetAlign software (Lommen 2009). Peak identification was performing using ChromaTOF (LEGO) and a library of TMS derivatized compounds from the Max Planck Institute for Molecular Plant Biology, Germany and validated with the TagFinder software (Luedemann et al 2008). Peak intensities were corrected for variations in the response of the internal standard and the exact mass of tissue extracted.

Statistical analysis of data

The experiments were carried out as a 2x2x2 factorial design (two accession, two CO_2 concentration and two supporting material) with five replicates, each replicate composed of on flask with three plants. Growth parameters data wew submitted to analysis of variance followed by tge Scott & Knott test (Scott and Knott 1974) at a significance leve of 5%. Experiment were performed two times to validate the data. To heatmap and hierarchical clustering analysis, PCA we Metabo analyst 3.0 software (Xia and Wishart 2016).

RESULTS AND DISCUSSION

In vitro growth of P. glomerata shoots is limited when grown on agar-based supporting medim

The growth of P. glomerata for both accessions was optimized by CO_2 enrichment (1000 µL L^{-1}) compared with the control (360 µL L^{-1}) (Table 1, Figure 1). The use of the Florialite® as support allowed greater plant lenght at the higher CO_2 concentration, whereas no growth differences were detected when agar was used Saldanha et al. (2014) reported that higher plant growth of P. glomerata was observed when grown in Florialite® and agar under CO_2 enrichment. In the present study, P. glomerata apexes were used, however, no differences in plant growth were observed in agar treatment. Variation in growth between apical and axillary buds was already studied in P. tuberosa by Flores et al. (2006), where it was observed a marked increase compared to apexes and nodal segments. Nicoloso and Erig (2002) pointed out the differences in in vitro growth between apexes and nodal segments of P. glomerata. However, no data were found regarding the influence of the support material and CO_2 enrichment.

In general, the higher growth with the CO_2 enrichment in the presence of Florialite® was expected, according to Saldanha et al. (2014) as the supplement with high CO_2 concentrations is related to the increase of photosynthetic rates and therefore carbon fixation (Kruger and Volin 2006). The growth is enhanced in the presence of a high porosity support as Florialite® (porosity close to 90%), unlike the agar, which has low porosity (Afreen-Zobayed et al 1999). The positive effects of CO_2-enriched supplement growth depend on the support porosity (Saldanha et al 2014). Plants grown in Florialite® developed more lateral roots from the main adventicous root that can optimize the nutrient absorption (Afreen-Zobayed et al. 1999). Florialite® have been used for propagation in large scale of important species like sugarcane (Xiao et al. 2011) and sweet potato (Zobayed et al. 1999).

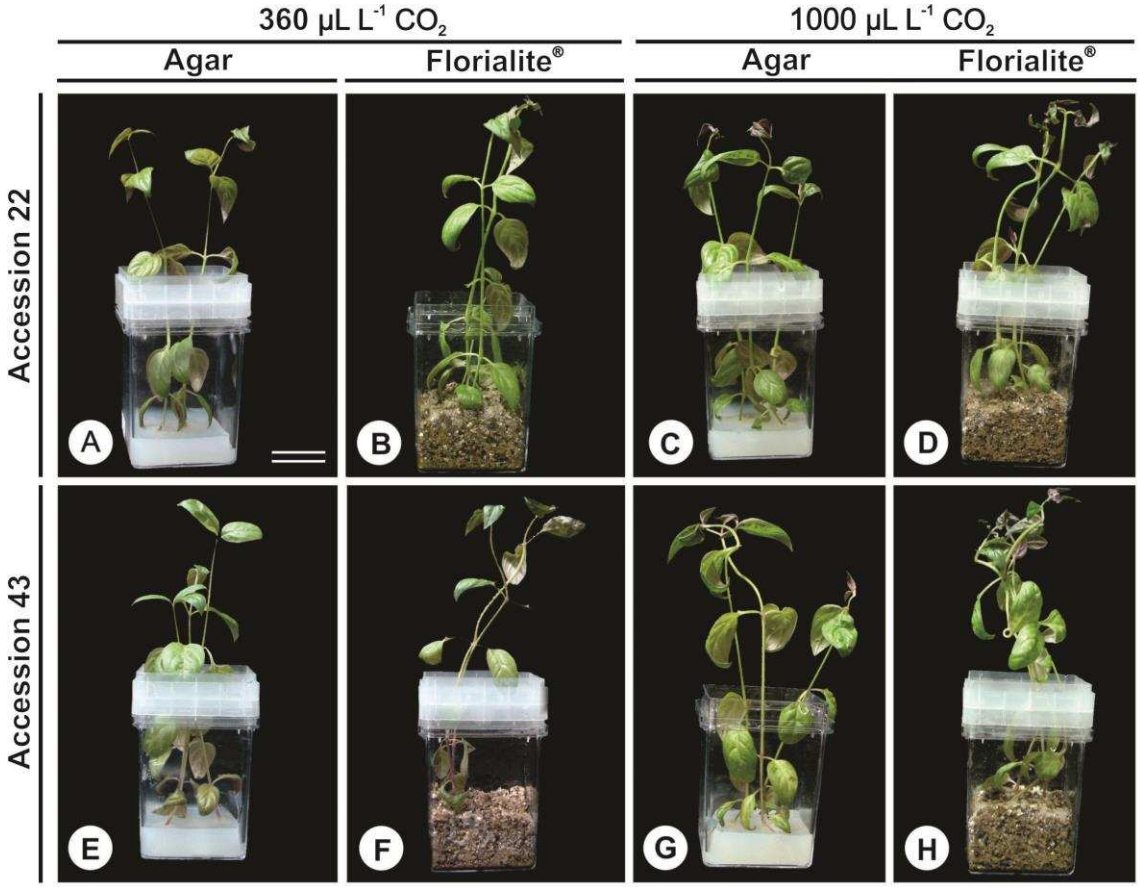

Figure 1. Magenta vessels holding 45-days in vitro grown plants of Pfaffia glomerata (Accessions 22 and 43) under CO_2 enrichment (360 ± 20 and 1000 ± 100 µL L^{-1} CO_2), and two supporting material for the explants (agar: first and third columns; and Florialite®: second and fourth columns). Barr: 3 cm.

Kozai and Cubota (2001) reported the importance of Florialite® on the promotion of photoautotrophic growth in several woods plants species in vitro (Acacia mangium, Coffea arabusta, Eucalyptus camaldulensis, Garcinia mangostana, Azadirachta indica, Paulownia fortune and Pinus radiata) associated with the increasing of CO_2 and light intensity in the vessels. Zobayed et al. (2004) in their review included Florialite® as a good choice for supporting material in photoautotrophic micropropagation systems. Florialite® has been still used for rapid cycling propagules of Medusagyne oppsitifolia, which have reduced genetic diversity due invasion and habitat clearance (Marriot and Sarasan 2010).

Table 1. Growth characteristics of two accessions of P. glomerata (Acession 22 and 43) propagated in vitro under CO_2 enrichment (360 and 1000 mol $^{-1}$ µM CO_2 air), in two supporting material (agar and Florialite®)

		Height (cm)			
		Supporting material		[CO_2] µL L^{-1}	
		Agar	Florialite®	360	1000
Accession	22	8.73 Bb	19.58 Ab	8.73 Bb	19.58 Ab
	43	17.71 Ba	21.50 Aa	17.71 Ba	21.50 Aa
Supporting material	Agar			13.39 Ab	13.05 Ab
	Florialite®			19.83 Ba	21.25 Aa
		Number of nodes			
		Supporting material		[CO_2] µL L^{-1}	
		Agar	Florialite®	360	1000
Accession	22	4 Ba	6 Aa	4 Ba	6 Aa
	43	4 Ba	6 Aa	4 Ba	6 Aas
Supporting material	Agar			4 Ab	5 Ab
	Florialite®			5 Ba	6 Aa
		Stem diameter (mm)			
		Supporting material		[CO_2] µL L^{-1}	
		Agar	Florialite®	360	1,000
Accessions	22	1.05 Ba	1.32 Aa	1.05 Ba	1.32 Aa
	43	1.26 Ba	1.26 Aa	1.26 Aa	1.56 Aa
Supporting material	Agar			1.17 Ab	1.14 Ab
	Florialite®			1.50 Aa	1.38 Aa

Means followed by the uppercase capital letters horizontally and, lowecase vertically dor not statistically different among them as assessed by the Scott and Knott's test at

the 5% probability level.

Leaf micromorphometrics under CO_2 enrichment increase in response to culture medium with high porosity

Photoautotrophic conditions led to an increase in leaf micromorphometric features in P. glomerata (Table 2, Figure 2). Plants grown under CO_2 enrichment had greater leaf area, midrib lenght, adaxial and abaxial perimeter, vascular bundle, and thicknesses of both sides, compared to the control. However, this was only when Florialite® was the support material. It is suggested that agar is a limiting factor in promoting Pfaffia glomerata growth in photoautotrophy system as demonstrated by growth and micromorphometric results. In this sense, the efficient promotion of P. glomerata growth in photoautotrophy system depends on an efficient supporting material for the explante like Florialite®, as demonstrated by Saldanha et al. (2014). In this study, besides the difference in plant growth, differences were found in the chloroplast lamellation pattern in P. glomerata leaves and changes in stomata size and density under CO_2 enrichment, that influenced plant growth.

In this study, the increase in leaf micromorphometrics corroborates the results found in Eucalyptus saligna leaves. The anatomical features increased at an enrichment of 650 $\mu L\ L^{-1}$ CO_2 and decreased in the presence of a high temperatures. Supporting material with agar has low porosity and may limit to obtaining resources for the plant compared to a higher porosity supporting material such Florialite®. It is known that plant leaves cultured photoautotrophically in vitro were anatomically affect by CO_2 enrichment and the supporting material (Kirdmanee et al. 1995). Thus, agar can affect essential cell wall enzymes such xyloglucan endotransglycosylase (XTH), which is responsible for cell expansion and there are studies demonstrating that CO_2 enrichment increases XTH activity (Ranasinghe and Taylor 1996).

Table 2. Leaf micromorphometrics of two accessions of P. glomerata (Accession 22 and 43) grown from explants cultured under different supporting material (agar and Florialite®) and CO_2 concentrations (360 and 1000 µL L^{-1})

		Leaf area (nm^2)			
		Accessions		[CO_2] µL L^{-1}	
		22	43	360	1000
[CO_2] µL L^{-1}	360	645 Aa	655 Aa		
	1000	676 Aa	623 Aa		
Supporting Material	Ágar	690 Aa	677 Aa	812 Ab	556 Bb
	Florialite®	630 Aa	578 Ab	465 Bb	744 Aa
		Adaxial leaf perimeter (µm)			
		Accession		[CO_2] µL L^{-1}	
		22	43	360	1,000
[CO_2] µL L^{-1}	360	4458 Aa	4525 Aa		
	1000	4515 Aa	45000 Aa		
Supporting Material	Ágar	4398 Bb	4569 Aa	4573 Aa	4395 Bb
	Florialite®	4575 Aa	4465 Aa	4420 Bb	4620 Aa
		Abaxial leaf perimeter (µm)			
		Accession		[CO_2] µL L^{-1}	
		22	43	360	10000
[CO_2] µL L^{-1}	360	4508 Aa	4690 Aa		
	1000	4683 Aa	4601 Aa		
Supporting Material	Ágar	4628 Aa	4659 Aa	4723 Aa	4566 Aa
	Florialite®	4562 Aa	4638 Aa	4483 Bb	4718 Aa
		Adaxial leaf thickness (µm)			
		Accession		[CO_2] µL L^{-1}	
		22	43	360	10000
[CO_2] µL L^{-1}	360	47 Aa	42 Ba		
	1000	48 Aa	33 Bb		
Supporting Material	Ágar	45 Ab	36 Ba	47 Aa	35 Bb
	Florialit	50 Aa	32 Ba	37 Bb	46 Aa

e®

		Abaxial leaf thickness (µm)			
		Accession		[CO_2] µL L^{-1}	
		22	43	360	1000
[CO_2] µL L^{-1}	360	41 Aa	35 Ba		
	1000	39 Aa	27 Bb		
Supporting Material	Ágar	39 Aa	30 Ba	39 Aa	31 Bb
	Florilite®	41 Aa	27 Ba	32 Bb	36 Aa

		Mesophyll thickness (µm)			
		Accession		[CO_2] µL L^{-1}	
		22	43	360	1000
[CO_2] µL L^{-1}	360	297 Aa	313 Aa		
	1000	321 Aa	292 Aa		
Supporting Material	Ágar	326 Aa	325 Aa	369 Aa	255 Bb
	Florilite®	293 Aa	272 Ab	207 Bb	358 Aa

		Midrib Area (nm^2)			
		Accession		[[CO_2] µL L^{-1}	
		22	43	360	1000
[CO_2] µL L^{-1}	360	2298 Aa	2694 Aa		
	1000	2596 Aa	1922 Aa		
Supporting Material	Ágar	2371 Aa	2766 Aa	3106 Aa	2031 Ba
	Florilite®	2522 Aa	1949 Ab	1985 Ab	2486 Bb

		Midrib length (µm)			
		Accession		[CO_2] µL L^{-1}	
		22	43	360	1000
[CO_2] µL L^{-1}	360	922 Bb	1029 Aa		
	1000	1136 Aa	700 Bb		
Supporting Material	Ágar	911 Ab	839 Ba	976 Aa	774 Bb
	Florilite®	1146 Aa	783 Ba	867 Bb	1062 Aa

		Vascular bundle Perimeter (µm)			
		Accession		$[CO_2]$ µL L^{-1}	
		22	43	360	1000
$[CO_2]$ µL L^{-1}	360	1234 Ab	1342 Aa		
	1000	1546 Aa	959 Bb		
Supporting Material	Ágar	1494 Aa	960 Bb	1264 Aa	1191 Aa
	Florialite®	1285 Ab	1137 Aa	1108 Ba	1314 Aa

Means followed by the uppercase capital letters horizontally and, lowecase vertically dor not statistically different among them as assessed by the Scott and Knott's test at the 5% probability level.

CO_2 enrichment on Florialite® enhanced the plastid differentiation in Pfaffia glomerata leaves

Ultrastructural changes were observed in P. glomerata chloroplasts (Ac 22) subjected to different CO_2 concentrations and supporting material for explant (Figure 3). Plants grown under Florialite® and 360 µL L^{-1} (Figure 3A) and 1000 µL L^{-1} (Figure 3C) showed large chloroplasts with an oval shape characteristic and thylakoid membranes clearly differentiated into grana stacks. Plants grown on agar in 360 µL L^{-1} (Figure 3B) and 1000 µL L^{-1} (Figure 3D) showed minor chloroplast, with normal shape, with smaller thylakoid membrane grana stacks. The plastoglobuli accumulation was observed in both treatments, as well as the absence of starch granules in the chloroplasts.

Ultrastructural changes similar to those observed in Ac 22 were observed in Pfaffia glomerata chloroplasts of Ac 43 subjected to different CO_2 concentrations and supporting material. Plants grown under Florialite® and 360 µL L^{-1} (Figure 4A) and 1000 µL L^{-1} (Figure 4C) showed larger chloroplasts with oval shape and differentiated lamellae thylakoid membranes with the formation of few grana stacks. Plants grown on agar in 360 µL L^{-1} (Figure 4B) and 1000 µL L^{-1} (Figure 4D) showed chloroplasts with standard format and apparently smaller tilakoid lamellation with the formation of few grana stacks. The plastoglobuli accumulation was observed in both treatments, as well as no starch granules in the chloroplasts. The higher number of plastoglobuli can be

related with the in the sense of mitigation of oxidative stress in the photosynthetic apparatus (Martins et al. 2008**)**.

This change in lamellation pattern of Pfaffia glomerata cloroloplasts was previouslly reported by Saldanha et al. (2014). However, no differences in chloroplast size were pointed out. Such differences may represent an improved surface area, leading to greater light energy capture (consistent with the higher pigment concentration under elevated CO_2) by the photosystems localized in membrane (Redondo-Gómez et al. 2010), which is vital to optimize CO_2 assimilation under high CO_2 conditions. CO_2-enriched atmosphere enhanced the plastid differentiation process up to mature chloroplasts with grana and intergranal thylakoids as demonstrated in Vargas-Suarez et al. (1995). Similar observations were previously reported in Platanus orientalis leaves (Velikova et al. 2009) and Solanum tuberosum (Sun et al. 2011) cultivated under elevated CO_2, and may represent adaptive changes at cellular level in response to environmental conditions (Mostowska 1997). These adaptive responses can be noticed here where the morpho-anatomical parameters were increased under enriched of CO_2 (Fig. 2). The treatment on agar do not allowed the differentiation of leucoplast on chloroplast in P. glomerata in both CO_2 concetration.

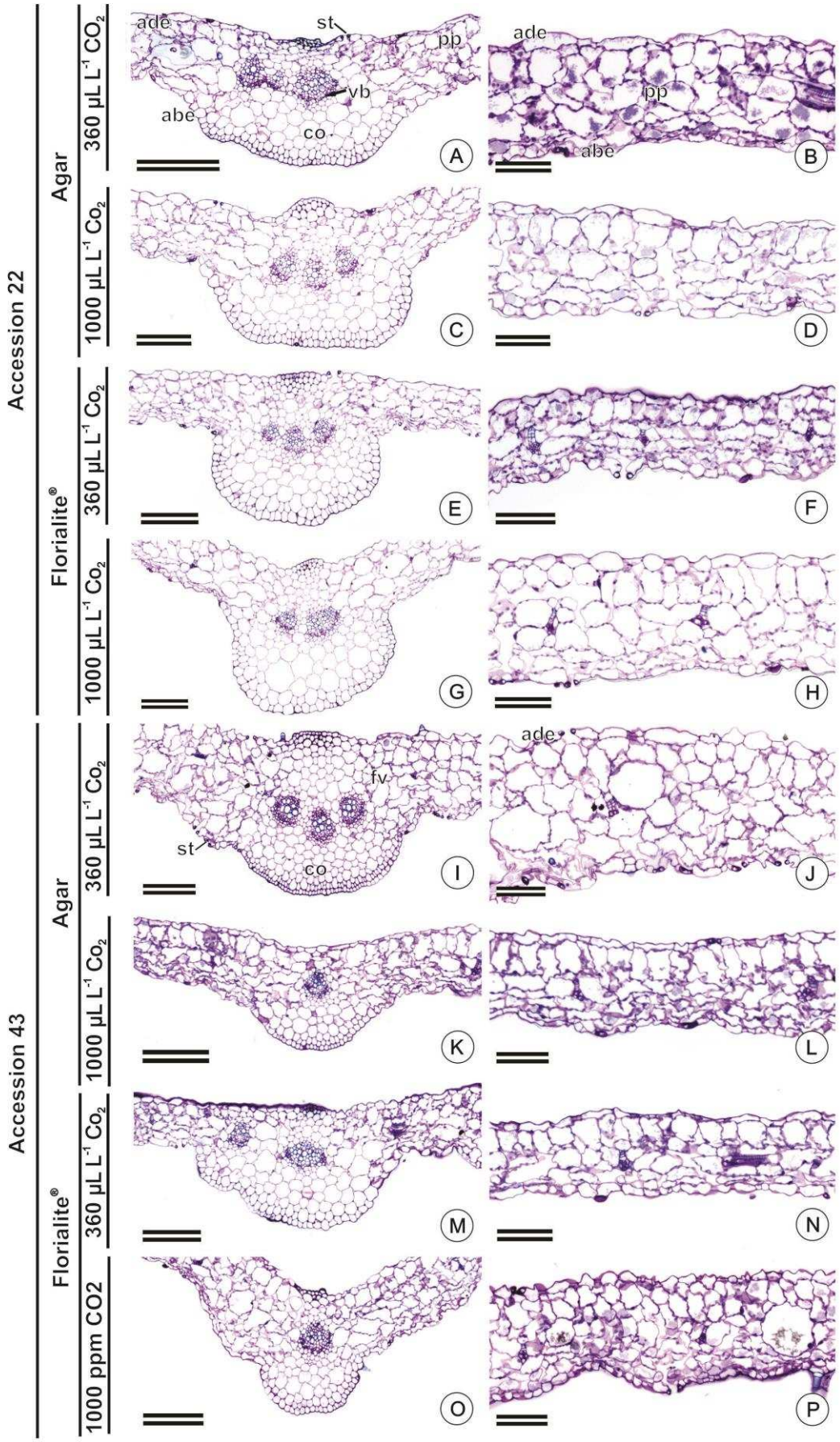
Accession 22
Accession 43
Agar
Florialite®
360 µL L-1 CO2
1000 µL L-1 Co2
1000 ppm CO2
ade
abe
pp
st
vb
co
fv
A
B
C
D
E
F
G
H
I
J
K
L
M
N
O
P

Figure 2. Leaf anatomical aspects of two accessions (22 and 43) of P. glomerata, cultivated in two supporting material (agar and Florialite®) and two CO_2 concentrations (360 and 100 µL L^{-1} CO_2). **Acession 22** (A-H). Cultivation in agar under 360 µL L^{-1} CO_2 (A-B) and 1000 µL L^{-1} CO_2 (C-D). Cultivation in Florialite®) under 360 µL L^{-1} CO_2 (E-F) and 1000 µL L^{-1} CO_2 (G-H). **Acession 43** (I-P). Cultivation in agar under 360 µL L^{-1} CO_2 (I-J) and 1000 µL L^{-1} CO_2 (K-L). Cultivation in Florialite® under 360 µL L^{-1} CO_2 (M-N) and 1000 µL L^{-1} CO_2 (O-P). ade: adaxial epidermis; abe: abaxial epidermmis; co: córtex; pp: palisade parenchyma; st stomata; vb vascular bundle. Bars A. C. E. G. I. K.M O: 300 µm. B.D. F.H. J. L. N. P: 100 µm.

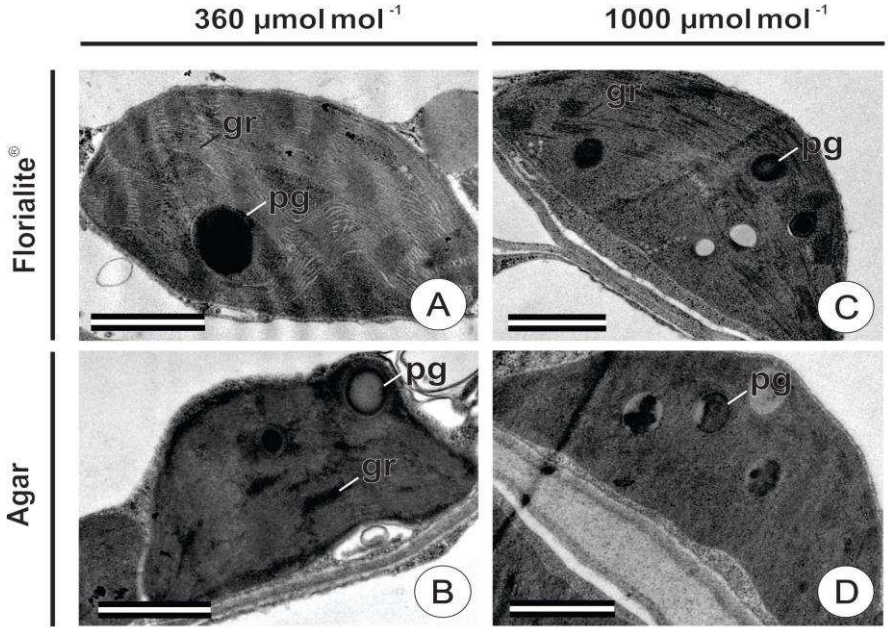

Figure 3. Ultrastructure of P. glomerata (Accession 22) chloroplasts grown in different concentrations of CO_2 and supporting material: A, C: Florialite. A) P. glomerata under 360 µL L^{-1} of CO_2. C) P. glomerata under 1000 µL L^{-1} of CO_2. B, D. Agar . B P. glomerata under 360 µL L^{-1} of CO_2. D. P. glomerata under 1000 µL L^{-1} of CO_2. pg: plastoglobuli ; gr: granum . Bars: 1 µm.

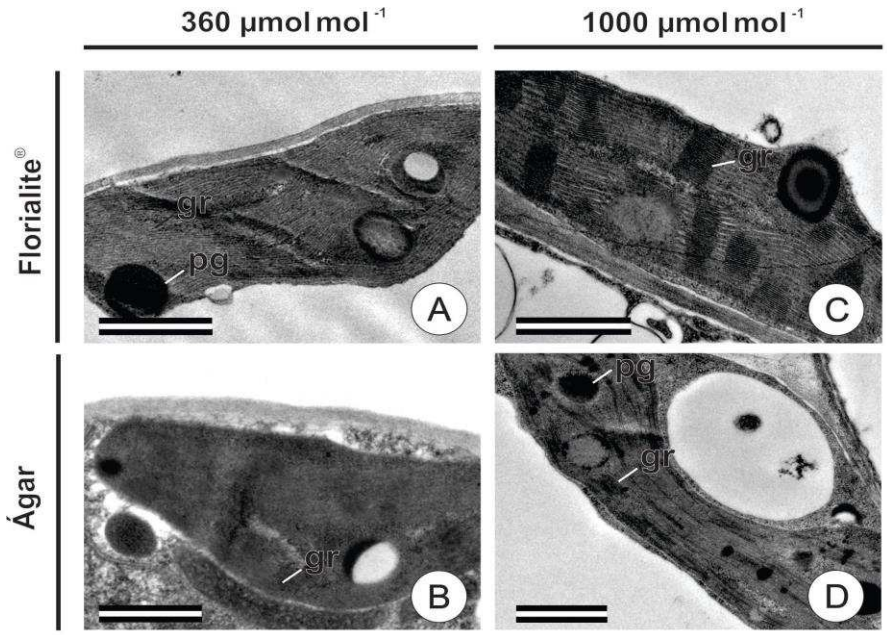

Figure 4. Ultrastructure of P. glomerata (Accession 43) chloroplasts grown in different concentrations of CO_2 (360 and 1000 µL L^{-1}) and supporting material (Agar and Florialite®): A, C: Florialite. A) P. glomerata under 360 µL L^{-1} of CO_2. C) P. glomerata under 1000 µL L^{-1} of CO_2. B, D. Agar . B P. glomerata under 360 µL L^{-1} of CO_2. D. P. glomerata under 1000 µL L^{-1} of CO_2. pg: plastoglobuli ; gr: granum. Bars = 1 µm.

Content of 20-hydroxyecdysone (20E) increases in plants in Florialite® under high CO_2 conditions

As shown in Table 3, the Ac 43 produced more 20E than Accession 22. However, both accessions increased 20E content on elevated CO_2 when grown in Florialite®. The highest 20E contente is related to a greater root aeration provided by Florialite® (Afreen-Zobayed et al 1999), compared to agar, promoting the secondary metabolites production (Saldanha et al. 2014). Similar results were found for Morinda citrifolia that produced higher secondary metabolites (anthraquinones, phenolics, and flavonoids) concentration when cultured in a more aerated medium (Ahmed et al. 2008) and elevated CO_2 modulates essential oil profile in Lippia alba (Batista et al. 2017).

According to Cruz (2011), Accession 43 has a higher 20E content in the shoot, while Ac 22 has a greater 20E content in the roots, whereas P. glomerata cultivated in agar does not provide a good root development, as observed in Florialite®. The Ac 43,

therefore, seems to respond better to 20E levels when grown on a support material that allows greater root and shoot development, like Florialite®.

Table 3. Concentration of 20E in the P. glomerata shoot (Accessions 22 and 43) 45-days grown under CO_2 enrichment (360 and 1000 µL L^{-1} of CO_2), and two supporting material for explant (agar and Florialite®).

		[20E] µL L^{-1}			
		Supporting material		[CO_2] µL L^{-1}	
		Agar	Florialite®	360	1000
Accession	22	53,31 Aa	49,70 Ab	53,31 Aa	49,70 Ab
	43	68,76 Ba	120,47 Aa	68,76 Bb	120,47 Aa
Supporting material	Agar			67,15 Aa	54,92 Ab
	Florialite®			55,91 Ba	114,25 Aa

Means followed by the uppercase capital letters horizontally and, lowecase vertically dor not statistically different among them as assessed by the Scott and Knott's test at the 5% probability level.

Metabolic profile shows the increasing of photosynthesis and their intermediaries by photoautotrophic system

Almost 50 metabolites were identified in in vitro culture conditions. They represented in a heatmap, where the metabolites in red are in higher relative concentrations and in blue are lower realtive concentrations (Figure 5). The triple factorial (2x2x2) was dismembered in double factorials presented in Tables 7, 8 and 9 in the annex.

The analysis demonstrated that enrichment with CO_2 and supporting material had impact on metablic profile, that corroborate with Badr et al. (2015). The relative amount of amino acids generally increased progressively in plants grown on agar in an atmosphere of 360 and 1000 µL L^{-1}. However, when Florialite® was used, glycine, glutamate and glutamine have also increased. The lack of sucrose in the medium causes a decrease in in vitro amino acid content due to the nitrogen abundance in the MS medium and also to the high availability of NH_4^+. This demonstrates the importance of in vitro plants in the assimilation of an abundant nitrogen amount in less reactive metabolites (Badr et al. 2015). The lower levels of amino acids in plants grown at high

CO_2, this could be the caused by an increase of the membrane permeability, which was higher in plants cultured under elevated CO_2, consequently leading to a greater resilience to water stress (Pérez-Jimenez et al 2015).

The increase of amino acid content in the treatments with agar and 360 µL L^{-1}, causes a decrease in the content of tricarboxylic acid cycle (TCA) intermediates citrate and fumarate. The reduction of these intermediate point to a redirection of 2-oxoglutarate and oxoglutarate, required for nitrogen assimilation (Sima et al. 2001).

Levels of sugars increased in treatment in 1000 µL L^{-1} of CO_2 in both accession of P. glomerata. CO_2 enrichment led to higher glucose, sucrose and starch contents, and showed decreased levels of photorespiratory intermediates such as glycolate, glycine, and glycerate and decreased levels of TCA cycle metabolites (e.g. succinate, fumarate, and malate), and a significant increase of maltose at both conditions. These results indicated low CO_2 (360 µL L^{-1}) had little effect on Calvin cycle and elevated CO_2 affected both Calvin cycle and respiratory activities in Pfaffia glomerata.

It has been observed that organic acids and amino acids showed the opposite tendency with the increase of CO_2 in the atmosphere (1000 µL L^{-1}) and using Florialite® in both accessions. This can be noticed mainly in organic acids related to the TCA cycle. Some compounds showed different behavior as the shikimic acid and ascorbate. It is known that the concentration of ascorbate in leaves is positively related to light intensity and participate in the acclimatization (Eskling and Akerlund 1998). The higher accumulation of ascorbate was observed in treatments with lower concentrations of CO_2 and less porous supporting material. Ascorbate plays an important role in the photosynthetic apparatus protection against adverse effects of light and photooxidative damage (Foyer et al. 2003).

Aromatic amines (dopamine, tyrosine, tryptophan and tyramine) and shikimate are precursors of metabolites (alkaloids and phenolics respectively) linked to abiotic and biotic stresses. Aromatic amines in general enhanced its content on Ac 22 in 360 and 1000 µmol CO_2 µL L^{-1} (in agar), and shikimate increased the content on Ac 43 in 1000 and 360 µL L^{-1} (agar). These findings reveal the environment more stressful for each access of P. glomerata and difference on stress sensibility of each accession. Elevated

CO_2 concentration provided carbon supply to the plant and phenolic synthesis was enhanced, leading to an increase in lignin (Richet et al 2012), proanthocyanidins and flavonols content (Lavola and Julkunen-Tiitto 1994; Ibrahin and Jaafar 2012), and indole alkaloid genes (Paudel et al. 2016).

There was a reduction of histidine, hydroxyproline, lysine, methionine, pyroglutamate, serine, tyrosine, threonine, tryptophan and ascorbate contents in P. glomerata grown in Florialite® and 1000 µL L^{-1}. In this experiment there was an increase in the urea amount in the treatments with 360 µL L^{-1} CO_2, and slightly porous support material (agar). Plants growing in little porous support material have low carbon fixation capacity associated with smaller gas exchange by low CO_2 availability. In this context, they adopt another strategy with excessive N content present in MS medium avoiding the possible toxicity for ammonia in the tissues. These responses represent an adaptation of plants in nitrogen assimilation while using the least possible carbon reserves (Badr et al. 2015).

Metabolic profiling evidences urea as a biomarker of photoautotrophic potential

Urea has a high rate of nitrogen: carbon (N: C, 2: 1) and is less toxic than ammonia and so can be used as storage compounds in plants. The higher urea levels were found in treatments with lower CO_2 availability or less porous supporting material, which in turn have limited photosynthetic capacity and insufficient availability carbon. This urea accumulation is as a good biomarker of insufficient light or low carbon fixation in vitro (Badr et al. 2011). This result confirms that in agar treatments urea accumulation evidenced the low capacity of carbon assimilation.

In this study there was a decrease of urea cycle intermediates content in treatments with high CO_2 and Florialite®. On the contrary, urea accumulated in treatment with low CO_2 concentration (360 µL L^{-1}) and supporting material is disadvantageous to photoautotrophy (agar). The same applies to ex vitro grown plants (autotrophic culture) when compared with plants grown in vitro, indicating that urea cycle is operational in plants under certain conditions (Badr et al. 2011).

Intermediaries involved in osmotic adjustment increase in photoautotrophic system

It was observed the accumulation of hydroxyproline, aspartate and myo-inositol in accession 43 grown in Florialite® in 360 or 1000 µL L^{-1} CO_2 and accession 22 grown in Florialite® in 360 µL L^{-1}. Myo-inositol increased the content in accession 22, on agar under 1000 µL L^{-1} CO_2. These molecules are known to be synthesized in response to abiotic stresses (Roessner-Tunali et al. 2003) and had the content increasing on high light (Obata and Fernie 2012). These results corroborate our results, evidencing the need for an osmotic adjustment in the photoautotrophic system in vitro mainly due to the high light irrandiance and may be responding to high osmotic potential in a medium rich of nitrogen and minerals and more porous supporting material. These molecules are involved in osmotic adjustment, stabilization of cellular structure, capturing free radicals and regulating the redox potential in stress situations (Cha-um and Kirdmanee 2008).

Accessions 22 and 43 of P. glomerata presents different behavior regarding the adjustment to stress tolerance as demonstrated by polyamine content

In vitro cultivated plants have large amounts of polyamines (Gill and Tuteja 2010. In this study putrescine showed different behavior between two accessions, accumulating in Ac 22 in treatments with Florialite® and 1000 µL L^{-1} and decreasing in Ac 43 in the same treatments. Interestingly, there is a parallel between the urea cycle and polyamine biosynthesis, where many urea cycle intermediates are required for the biosynthesis of polyamines. Putrescine is directly produced from ornithine decarboxylase by ornithine or indirectly by arginine decarboxylase arginine (Martin-Tanguy 2001). The presence of putrescine may indicate activation polyamine biosynthesis pathway on in vitro conditions and the dichotomy between the accession may indicate distinct adjustment to stress tolerance (Gill and Tuteja 2010). Ac 22 in this sense seems to have less tolerance to stress, because they acumuled polyamine in environmental little stressful for Ac 43. Putrescine have been reporter to be increased upon exposure to alternative stress conditions (Boone et al. 2017).

The first two components (PC1 and PC2) explained 87.9% of the total variance among the data (Fig 6). PC1 accounts for 82% of the total variance and PC2 5.9%. The PCA biplot demonstrate that plants cultured in photoautrophic conditions were much different from those cultured in photoheterotrophic system. A closer examination of the profile of the these plants reveals three patterns: 1. Accession in which the photoautrophy was optimized by the supporting material; 2. Accessions in which the supporting material did not influence photoautrophy; 3. Photoautrophy limited by the supporting material used (Groups comprised into elipses on Figure 6).

A hierarchical cluster analysis was performed in a dendrogram of metabolites based on significant differences of relative abundance (Figure 7). Two well-defined groups are highlighted, one good photoautotrophy group and another one with poor photoautotrophy competence. In vitro conditions alter the overall metabolism as observed in the hierarchical cluster analysis and PCA. Treatments with 360µL L^{-1} CO_2 or agar as supportig material were grouped into poor photoautotrophic potential group.

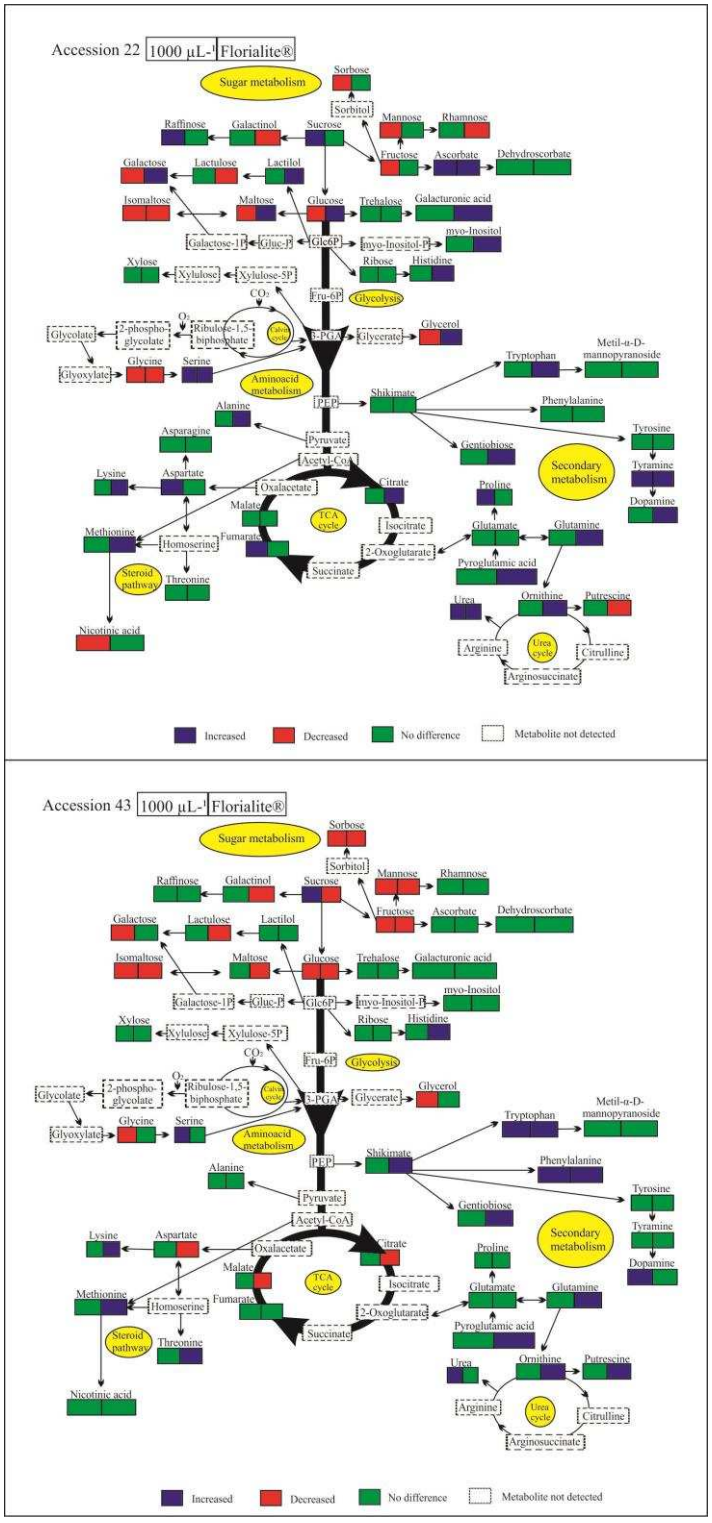

Figure 5. Schematic showing significant variations of the metabolites abundance mapped onto the metabolic netwok: Colored boxes indicate changes in particular metabolite in the Acession 22 and Acession 43 of Pfaffia glomerata under CO_2 enrichment (1000 µL L^{-1}) and Florialite®.

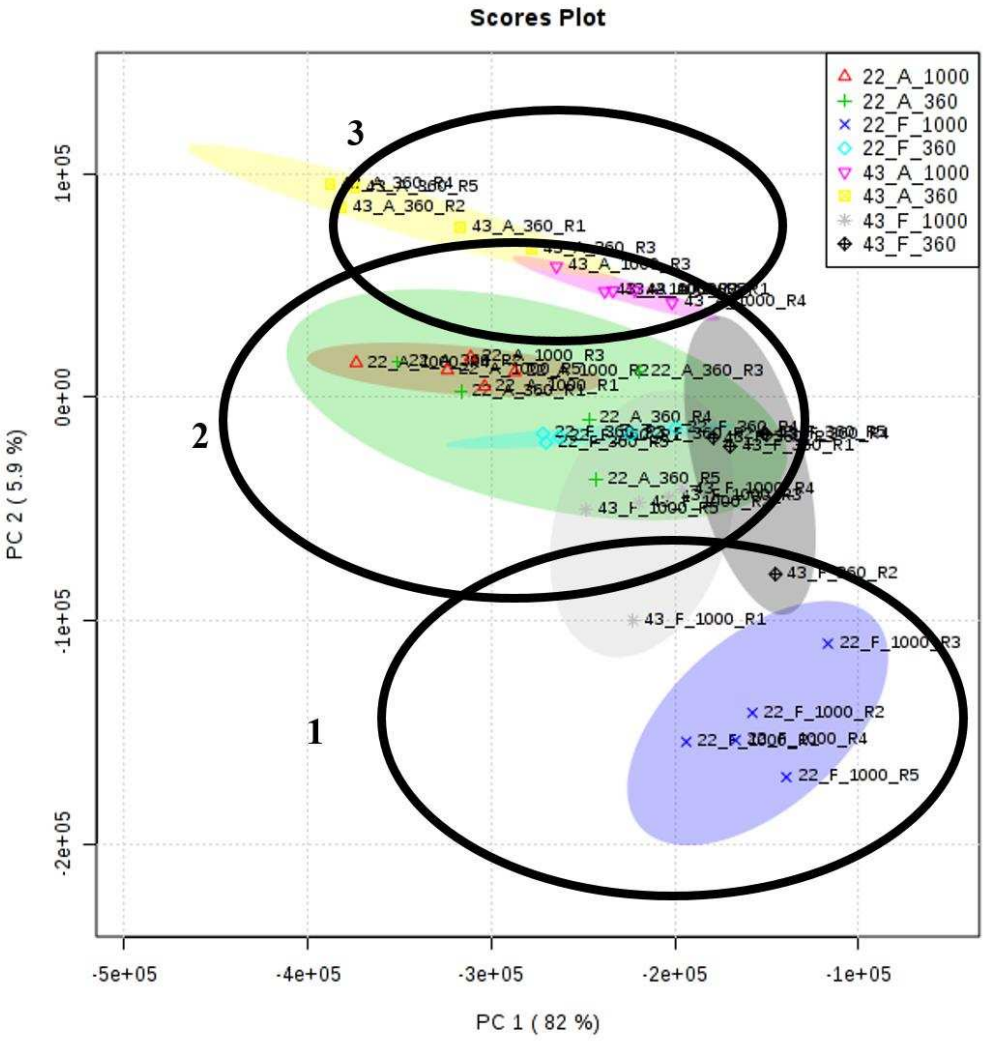

Figure 6. Two principal components of accessions 22 and 43 of Pfaffia glomerata grown under CO_2 enriched atmosphere (360 or 1000 µmol CO_2 µL L^{-1}) of supporting material for explant (agar or Florialite®). Ellipses represent groups formed: 1) photoautotrophy optimized by the supporting material; 2) supporting material did not influence photoautotrophy and 3) photoautotrophy limited by the supporting material.

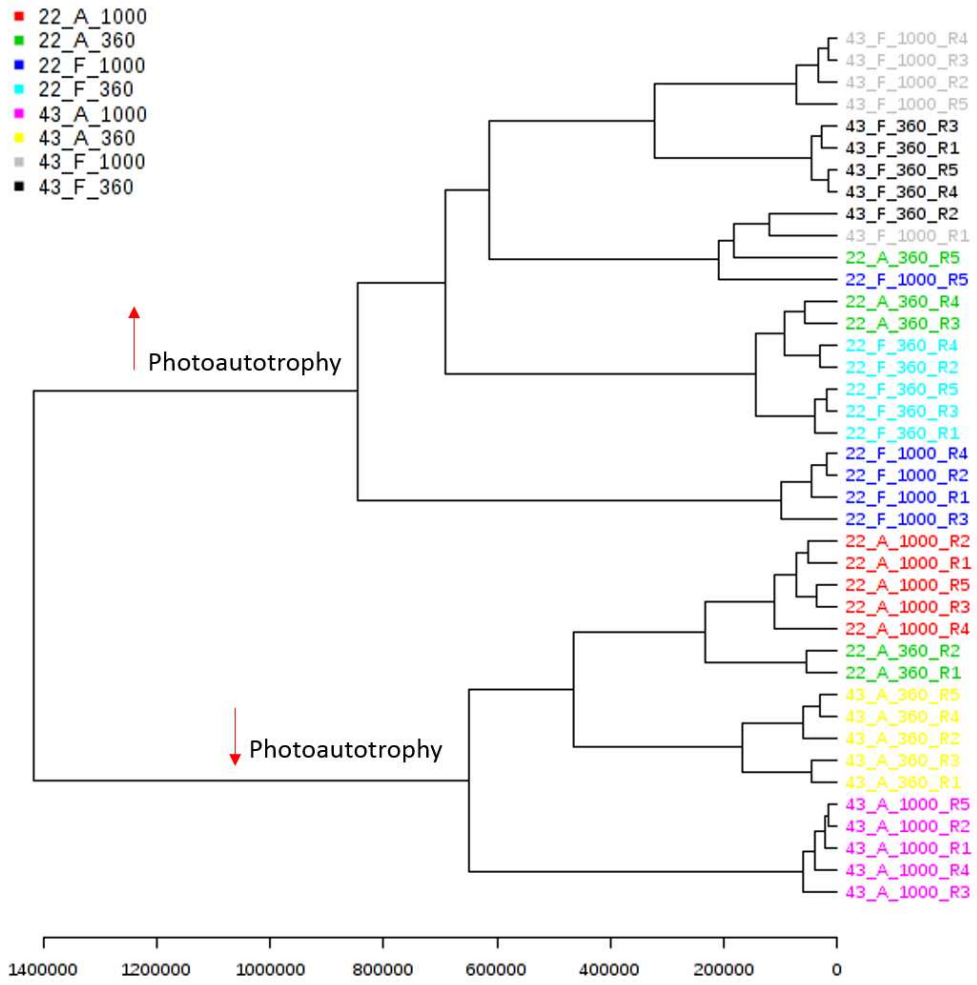

Figure 7. Grouping in a hierarchical dendrogram analysis of metabolites based on the significant differences in the relative abundance of accessions 22 and 43 of P. glomerata cultured in CO_2 enriched atmosphere (360 and 1000 µL L^{-1} CO_2 in two supporting material for the explants: Florialite®:F or agar:A). Five replications were used per treatment.

CONCLUSION

In conclusion, our results show that enrichment with CO_2 and supporting material had great influence on in vitro performance of Pfaffia glomerata by enhanced plastid differentiation in mature chloroplasts, and increasing 20-hydroxyecdysone content. The concentration of 1000 µL L^{-1} and Florialite® enhanced on photosynthesis intermediaries levels (amino acids, sugars, TCA), and stress- (aromatic amines and shikimate), osmotic adjustment-related compouds (hidroxyproline, aspartate and myo-inositol). Markedly, urea seems to be a biomarker of low photoautotrophic and Ac 22 seems to have less tolerance to stress than Ac 43, indicated by the polyamine content.

The results presented here are important for demonstrating key primary metabolites in the photoautotrophic development of P. glomerata in vitro. The work shows the importante metabolites associated with osmotic adjustment, nitrogen assimilation, stress tolerance and secondary metabolism modulated by CO_2 concentration and the differences in metabolisms between two accessions (22 and 43) of P. glomerata. In the latter case, the data is important for the germoplasm bank of P. glomerata and future works with accessions 22 and 43. Another important data presented here is the dependence of the photoautotrophy of an appropriate explant supporting material such as FLorialite®, already reported by Saldanha et al (2012, 2013 and 2014) and studied at the metabolic level in this study. This directly reflects the in vitro development of P. glomerata in the culture media to be used and ex vitro metabolites to be used in order to increase the development and production of 20-hydroxyecdysone.

REFERENCES

Afreen-Zobayed F, Zobayed SMA, Kubota C, Kozai T, Hasegawa O (1999) Supporting material affects the growth and development of in vitro sweet potato plantlets cultured photoautotrophically. **In Vitro Cell Dev Biol Plant**, 35:470–474.

Ahmed S, Hahn EJ, Paek K (2008) Aeration volume and photosynthetic photon flux affect cell growth and secondary metabolite contents in bioreactor cultures of Morinda citrifolia. **J Plant Biol**, 51:209–212.

Badr A, Angers P, Desjardins Y (2011) Metabolic profiling of photoautotrophic and photomixotrophic potato plantlets (Solanum tuberosum) provides new insights into acclimatization. **Plant Cell Tiss Organ Cult**, 107:13-24.

Badr A, Angers P, Desjardins Y (2015) Comprehensive analysis of in vitro to ex vitro transition of tissue cultured potato plantlets grown with or without sucrose using metabolic profiling technique. **Plant Cell Tiss Organ Cult,** 122:491-508

Batista DS, Castro KM, Koehler AD, Porto BN, Silva AR, Souza VC, Teixeira ML, Cardoso MG, Santos MO, Viccini LF, Otoni WC (2017) Elevated CO_2 improves growth, modifies anatomy, and modulates essential oil qualitative production and gene expression in Lippia alba (Verbenaceae). **Plant Cell Tiss Organ Cult,** 128:357-368.

Bernard B, Gautier B (2005) **Use of ecdysteroids for preparing dermatological or cosmetological anti-hair loss compositions.** United States Patent, US 0137175 A1

Boone CHT, Grove RA, Adamcova D, Seravalli J, Adamec J (2017) Oxidative stress, metabolomics profiling, and mechanism of local anesthetic induced cell death in yeast. **Redox Biology**, 12:139-149.

Cha-Um S, Chanseetis C, Chintakovid W, Pichakum A, Supaibulwatana K (2011) Promoting root induction and growth of in vitro macadamia (Macadamia tetraphylla L. 'Keaau') plantlets using CO_2-enriched photoautotrophic conditions. **Plant Cell Tiss Organ Cult**, 106:435–444.

Eskling M, Akerlund HE (1998) Changes in the quantities of violaxanthin de-epoxidase, xanthophylls and ascorbate in spinach upon shift from low to high ligh. **Photosynth Res**, 57:41-50.

Fernandes JFO, Brito LC, Frydman JNG, Santos-Filho SD, Bernardo- FilhoM (2005) An aqueous extract of Pfaffia sp. does not alter the labeling of blood constituents with technetium-99m and the morphology of the red blood cells. **Rev Bras Farmacogn**, 15:126–132

Festucci-Buselli RA, Contim LAS, Barbosa LCA, Stuart JJ, Otoni WC (2008) Biosynthesis and potential functions of the ecdysteroid 20-hydroxyecdysone – a review. **Botany**, 86: 978-987.

Flores R (2006) **Cultura de tecidos e produção de ecdisona em Pfaffia glomerata e Pfaffia tuberosa (Amaranthaceae).** Tese (Doutorado em Agronomia). Universidade Federal de Santa Maria.Rio Grande do Sul.

Foyer CH, Noctor G (2003) Redox sensing and signaling associated with reactive oxygen in chloroplasts, peroxisomes and mitochondria. **Physiol Plant**, 119:655-364.

Gill SS, Tuteja M (2010) Polyamines and abiotic stress tolerance in plants. **Plant Signal Behav**, 5:26-33.

Higuchi ML (2011) **Compositions for inhibiting atherosclerosis**.United States Patent, US 7914781 B2

Iarema L, Cruz ACF, Saldanha CW, Dias LLC, Fontes RV, Oliveira EJ, Otoni WC (2012) Photoautotrophic propagation of Brazilian ginseng [Pfaffia glomerata (Spreng.) Pedersen]. **Plant Cell Tiss Organ Cult** , 110:227-238.

Ibrahim MH, Jaafar HZ (2012) Impact of elevated carbon dioxide on primary, secondary metabolites and antioxidant responses of Eleais guineensis Jacq. (oil palm) seedlings. **Molecules**, 17:5195-5211.

Kamada T, Picoli EAT, Vieira RF, Barbosa LCA, Cruz CD, Otoni WC (2009) Viariação dos caracteres morfológicos e fisiológicos de populações naturais de Pfaffia glomerata (Spreng.) Pederson e correlação com a produção de β-ecdisona. **Rev Brasil Plantas Med**, 11:247-256.

Karnovsky M J (1965) A formaldehyde-glutaraldehyde fixative of high osmolality for use in electron microscopy. **J Cell Biol**, **Plants**, 10: 188-204.

Kozai T, Kubota C (2001) Developing a Photoautotrophic Micropropagation System for Woody Plants. **J Plant Res,** 114: 525-537.

Kirdmanee C, Kitaya Y, Kozai T (1995) Effects of CO_2 enrichment and supporting material in vitro on photoautotrophic growth of Eucalyptus plantlets in vitro and ex vitro, **In Vitro Cell Dev Biol Plant,** 31:144-149.

Kruger LC, Volin JC (2006) Reexamining the empirical relation between plant growth and leaf photosynthesis. **Functional Plant Biol**, 33:421–429.

Lavola A, Julkunen-Tiito R (1994) The effect of elevated carbon dioxide and fertilization on primary and secondary metabolites in birch, Betula pendula (Roth). **Oecologia**, 99:315-321.

Lisec J, Shauer N, Kopka J, Willmitzer L, Fernier, AR (2006) Gas chromatography mass spectrometry-based metabolite profiling in plants. **Nature Prot,** 1: 387-396

Loizou NC (2009) **Health supplement**. United States Patent, US 0110674 A1, 2009

Lommem A (2009) MetAlign: interface-driven, versatile metabolomics tools for hyphenated full-scan mass spectrometry data processing. **Anal Chem** 81:3079-3086.

Luedemann A, Strassburg K, Erban A, Kopka J (2008) Tag Finder for the quantitative analysis of gas chromatogreaphy-mass spectrometry (CG-MS)-based metabolite profiling experiments. **Bioinformatics** 24:732-737.

Marriot P, Sarasan V (2010) Novel micropropagation and weaning methods for the integrated conservation of a critically endangered tree species, Medusagyne oppositifolia. **In Vitro Cell Dev Biol Plant**, 46:516-523.

Martins S, Machado SR, Alves M (2008) Anatomia e utra-estrutura foliar de Cyperus maritimus Poir. (Cyperaceae): estratégias adaptativas ao ambiente de dunas litorâneas. **Acta Bot Bras**, 22: 493-503.

Martins JPR, Verdoodt V, Pasqual M, De Proft M (2016) Physiological responses by Billbergia zebrina (Bromeliaceae) when grown under controlled microenvironmental conditions. **Afr J Biotechnol**, 15:1952-1961.

Martin-Tanguy J (2001) Metabolism and function of polyamines in plants: recent development (new approaches). **Plant Growth Regul**, 34:135-148.

Mendes FR (2011) Tonic, fortifier and aphrodisiac: adaptogens in the Brazilian folk medicine. **Rev Brasil Farmacogn**, 21:754–763.

Misra BB, Chen S (2015) Advances in understanding CO2 responsive plant metabolomes in the era of climate change. **Metabolomics,** 11:1478-1491.

Mostowska A (1997) Environmental factors affecting chloroplasts. In: Pessarakli M (ed) **Handbook of photosynthesis.** Marcel Dekker, New York, pp 407–426

Mroczek A (2015) Phitochemistry and bioactivity of triterpene saponins from Amaranthaceae Family. **Phytochemistry,** 14:577-605.

Murashige T, Skoog F (1962) A revised medium for rapid growth and bioassays with tobacco tissue cultures. **Physiol Plant**, 15: 473-497.

Neto AG, Costa JMLC, Belati CC, Vinholis AHC, Possebom LS, Silva Filho AA, CunhaWR, Carvalho JCT, Bastos JK, Silva MLA (2005) Analgesic and anti-inflammatory activity of a crude root extract of Pfaffia glomerata (Spreng) Pedersen. **J Ethnopharmcol**, 96:87–91

Nicoloso FT; Erig AC (2002) Efeito do tipo de segmento nodal e tamanho do recipiente no crescimento de plantas de Pfaffia glomerata in vitro. **Ciência Agrotecnol**, Edição especial, p.1499-1506.

Obata T, Fernie AR (2012) The use of metabolomics to dissect plant responses to abiotic stresses. **Cell Mol Life Sci,** 69: 3225-3243.

O'Brien TP, McCully ME (1981) **The study of plant structure principles and selected methods**. 1st edn. (Termarcarphi Pty: Melbourne) 14: 357.

Olalde JA (2008) **Multiple sclerosis synergistic phyto-nutraceutical composition**. United States Patent, US 0081046 A1

Paudel JR, Amirizian A, Krosse S, Giddings J, Ismail SAA, Xia J, Gloer JB, Dam NM, Bede JC (2016) Effect of atmospheric carbon dioxide levels and nitrate fertilization on glucosinolate biosynthesis in mechanically damaged Arabidopsis plants, **BMC Plant Biol**, 16:68. doi: 10.1186/s12870-016-0752-1.

Pérez-Jímenez M, López-Perez AJ, Otalora-Alcon G, Marin-Nicolas D, Piñero MC, Amor FM (2015) A regime of high CO_2 concentration improves the acclimatization process and increases plant quality and survival. **Plant Cell Tiss Organ Cult**, 121:547-557.

Pott A, Pott VS (1994) **Plantas do pantanal**. Embrapa-SPI, Corumbá.

Ranasinghe S., Taylor G (1996) Mechanism for increased leaf growth in elevated CO_2. **J Exp Bot,** 47:349-358.

Rangel JAO (2008) **Menopause disorder synergistic phyto-nutraceutical composition.** United States Patent, US 7381432.

Redondo-Go´mez S, Mateos-Naranjo E, Moreno FJ (2010) Physiological characterization of photosynthesis, chloroplast ultrastructure, and nutrient content in bracts and rosette leaves from Glaucium flavum. **Photosynthetica**, 48:488–493

Reynolds ES (1963) The use of lead citrate at high pH as an electronopaque stain in electron microscopy. **J Cell Biol**, 17:208–212.

Richet N, Afif D, Tozo K, Pollet B, Maillard P, Huber F, Priault P, Banvoy J, Gross P, Dizengremel P, Lapierre C (2012) Elevated CO_2 and/or ozone modify lignification in the wood of poplars (Populus tremula x alba). **J Exp Bot**, 63: 4291-4301.

Roessner-Tunali U, Hegemann B, Lytovchenko A, Carrari F, Bruedigm C, Granot D, Fernie AR (2003) Metabolic profiling of transgenic tomato plants overspressing hexokinase reveals that the influence of hexose phosphorylation diminishes during fruit development. **Plant Physiol Biochem**, 133:84-99.

Saldanha CW, Otoni CG, Azevedo JLF, Dias LLC, Rêgo MM, Otoni WC (2012) A low-cost alternative membrane system that promotes growth in nodal cultures of Brazilian ginseng [Pfaffia glomerata (Spreng.) Pedersen]. **Plant Cell Tiss Organ Cult**, 110:413-422.

Saldanha CW, Otoni CG, Notini MN, Kuki KN, Cruz ACF, Neto AR, Dias LLC, Otoni WC (2013) A CO_2-enriched atmosphere improves in vitro growth of Brazilian ginseng [Pfaffia glomerata (Spreng.) Pedersen]. **In Vitro Cell Dev Biol Plant**, 49:433-444.

Saldanha CW, Otoni CG, Rocha DI, Cavatte PC, Detmann KSC, Tanaka FAO, Dias LLC, DaMatta FM, Otoni WC (2014) A CO_2-enriched atmosphere and supporting material impact the growth morphophysiology and ultrastructure of in vitro Brazilian – ginseng [Pfaffia glomerata (Spreng.) Pedersen] plantlets. **Plant Cell Tiss Organ Cult**, 118:87-99.

Shibuya T, Ario T, Fukuda S (2001). **Composition**. United States Patent, US 6224872, 2001.

Scott RJ, Knott M (1974) A cluster analysis method for grouping means in the analysis of variance. **Biometric** 30:507-512.

Sun ZP, Li TL, Liu YL (2011) Effects of elevated CO_2 applied to potato roots on the anatomy and ultrastructure of leaves. **Biol Plant**, 55:675–680.

Vargas-Suarez M, Rincón-Guzman, Mújica-Jimènez C, Muñoz-Clares Ra, Jiménez SE (1996) Influence of carbon source and CO_2-enrichment on biochemichal parameters associated with photomixotrophia in maize callus cultures. **J Plant Phisiol**, 140: 585-591.

Xia, J. and Wishart, D.S. (2016) Using MetaboAnalyst 3.0 for Comprehensive Metabolomics Data Analysis. **Current Protocols in Bioinformatics,** 55:14.10.1-14.10.91.

Xiao Y, Niu G, Kozai T. Development and application of photoautotrophic micropropagation plant system. **Plant Cell Tiss Organ Cult**, 105: 149-158, 2011.

Zobayed SMA, Kubota C, Kozai T (1999) Development of a Forced Ventilation Micropropagation System for Large-Scale Photoautotrophic Culture and Its Utilization in Sweet Potato. **In Vitro Cell Dev Biol Plant**, 35:350-355.

Kozai T (2010) Photoautotrophic micropropagation - Environmental control for promoting photosynthesis. **Prop Ornam**

CHAPTER 2

Haloween genes expression and metabolite signature on the pathosystem root-knot nematode (Meloidogyne javanica) and Pfaffia glomerata

ABSTRACT

Pfaffia glomerata is a plant whose importance comes to constituent active 20-hydroxiecdysone (20E), that is the most important compound extracted from roots. This steroid presents therapeutic properties for the treatment of diabetes and haemorrhoids, besides having bioenergy, tonic and aphrodisiac effects and the 20E content can increased by root-knot nematodes of genus Meloidogyne. Comparison of the biosynthesis of ecdysteroids involved in insect molting, with the one occurring in plants, is an important tool on the regulation and mode of action in plants. The aim of this work is verify the effect of P. glomerata (Accessions 22 and 43) interaction with M javanica on 20E contente, changes on primary metabolismo and expression of Halloween. We analyzed metabolomics and expression of Spook and Phantom genes in leaves of both accessions inoculated and non-inoculated with M. javanica by CG-MS and RT-qPCR analyses respectively. 20E content in P. glomerata increased with presence of M. javanica. Metabolomics profile analysis showed us differences between the accessions 22 and 43. Pathosystem root-knot nematode and Pfaffia glomerata is related to compounds associated with galls development (citric acid), nematoide nitrogen nutrition (aminoacids), P. glomerata nitrogen cycle (aminoacids), plant-microorganism interaction (trehalose) and stress environment (sugars). The Halloween genes (Phantom and Spook) present only in insects were expressed in P. glomerata and is influenced by nematode-interaction, increasing expression on Ac 43 infected by nematode and increasing content of 20E. Conversely, Phantom and Spook were downregulated by the increase of 20E content in Ac 22. The root-knot nematode interaction causes root damage-induced 20E accumulation and by modulate of Phantom and Spook genes. The interaction triggers differences on specific primary metabolites in accessions of Pfaffia glomerata. Here is the first work of Halloweeng genes expression in plants.

Keywords: nematodes, ecdysone, Halloween genes, Brazilian ginseng, metabolomics

INTRODUCTION

Pfaffia glomerata (Amaranthaceae) commonly known as Brazilian ginseng, has great economic medicinal value due to accumulate the phytoecdysteroid 20-hydroxyecdysone (20E) (Lafont and Dinan 2003) and had saponins in high concentrations (Vardanega et al. 2017) that could have be involved in biochemical and physiological processes in plant and insects (Festucci-Buselli et al. 2008).

The ecdysteroids are steroid hormones found in arthropods (zooecdysteroid) and plants (phytoecdysteroid). The plants are capable of producing phytoecdisteroids from mevalonic acid (Alves et al. 2010). Nematodes belong to the clade Ecdysozoa therefore is likely to have hormonal regulation similar to the insect to molt (Dinan et al. 2009).

There are also many nematode species which are parasitic to plants. Decraemer and Hunt (2006) characterized 4,100 species of nematodes as plant parasites, which can infect a range of crop plants like wheat, soybean, potato, tomato, and sugar beet etc. Nematode infection can result in different above-ground symptoms in plants such as leaf chlorosis, patchy and stunted growth, wilting and susceptibility to other pathogens (Webster 1995).

The member of genus Meloidogyne are known as root-knot nematodes, which induce feeding structures called “galls”, each of which comprises of several giant cells (Jones and Payne 1978). However, the presence of these nematodes generated 20E increased content of different accessions Pfaffia (Iarema 2008). This may be correlated to possible existing positive interaction between the development of nematode and the production of the active compound in the plant, since it is analogous 20E of hormones involved in molting (Dinan et al. 2009).

Comparison of biosynthesis of ecdysteroids involved in insect moulting, with plants is an important tool on the regulation and mode of action in plants (Festucci-Busceli et al. 2008). The ecdysteroids are involved in several stages of the cycle of arthropods, in the regulation of molting, metamorphosis, development, reproduction. In insects, the protoracid glands secrete the ecdysone which is subsequently transformed into 20E (Buszczak and Segraves 2000). The cytochrome P450 enzymes encoded by the Halloween genes – spook (spo), phantom (phm), disembodied (dib), shadow (sad), and shade (shd) – catalyze a series of hydroxylation steps resulting in the active molting hormone 20-hydroxyecdysone (20E) (Zhou et al. 2016). Several plants are known to

synthetize 20E (Lafont et al. 2005), however no data presently indicate the ocurrence of the Halloween genes in plants and insect-like plant genes are suggested in order to encodes the hydroxylation enzymes of ecdysone in plant (Alekseeva 2004). The only reports on CYP enzymes (similar to Halloween genes) involved in phytoecdysteroid biosynthesis concern the C20-hydroxylase (Canals et al. 2005). This implies that plants by convergent evolution have envolved 20E biosynthesis as a defense mechanism against herbivorous insects (Bakrin et al. 2009).

The accumulation in 20E concentration occurs throughout the life of the plant, but due to distribution within the plant, its may change during ontogeny (Dinan et al. 2009) and build for example, the root system (Festucci-Buselli et al. 2008), which leads us to establish a relationship between the production location and the damage caused, both the root system and the aerial part of the species.

In view of the nematodes parasitizing the roots of Pfaffia, the local extraction of a substance used in the production of pharmaceuticals (Gomes 2010), and that the presence of these produced increased 20E content in different Pfaffia accession, Cruz (2011) evaluated accessions of this plant for resistance to root-knot nematodes, and found that the presence of these nematodes influence the content of the accumulation of the active ingredient (20E). So, the Ac 43 responds better to aeration and has higher content of 20E in the shoot compared to the Accession 22 that has roots with higher content of 20E. According to Cruz (2011) and Iarema (2008) suggest that accession 22 is suscetible to nematodes while the 43 is tolerant.

The combination of metabolite profiling, multivariate data mining and expression genes is a powerful approach to classify samples and to reveal key metabolites and pattern responsible for specific processes (Scherling et al. 2009). Desbrosses et al. (2005) established protocols for analysis of metabolomics for the study of plant-microbe interactions. Therefore, we applied these technology to verify the effect of the interaction of nematode on the 20E production in accession 22 and 43 of Pfaffia glomerata, the metabolic alterations and halloween genes expression.

MATERIALS AND METHODS

Obtainment the inoculum of Meloidogyne javanica

To obtain the nematode inoculum, populations of Meloidogyne javanica, previously grown in tomato (Solanum lycopersicon ' Santa Clara') roots were used. Tomato plants were kept in vessels with 1.5 L capacity, containing soil and sand in the ratio 1:1 (v/v) and kept in a greenhouse. The nematode eggs were extracted following Boneti and Ferraz (1981) method and the concentration is determined in Peters blades under an optical microscope, following.

Plant material

It was used as plant material two P. glomerata accessions (Ac 22 and Ac 43) propagated in vitro from shoot tips on MS medium consisting of salts (Murashige and Skoog 1962), MS vitamins (0.5 mg L^{-1} nicotinic acid 0.5 mg L^{-1} piridoxina.HCl , 0.1 mg L^{-1} thiamine. HCl and 2 mg L^{-1} glycine) and 100 mg L^{-1} myo-inositol). The culture medium had pH adjusted to 5.7 and gelled with 7 g L^{-1} agar granules (Merck®, Germany) and subsequently sterilized by autoclaving at 121 ° C and 1.5 atm for 15 min .Cultures were maintained at 25 ± 2 ° C under irradiance of 150 µmol m^{-2} s^{-1} and a photoperiod of 16 h.

Subsequently, the plantlets (average 25 days-old) were acclimatized with split-roots system in hydroponics with the following macronutrients: KNO_3 (101.10 mg.dm^{-3}), $MgSO_4.7H_2O$ (27.11 mg.dm^{-3}), $Ca(NO_3)_2.4H_2O$ (188.93 mg.dm^{-3}) and $NH_4H_2PO_4$ (42.56 mg.dm^{-3}), remaining in culture for 15 days. After growing hydroponically, plants were transferred to pots with 1.5L capacity, containing soil and sand in the ratio 1:1 (v/v), kept in the greenhouse.

M. javanica inoculation of nematode-free Pfaffia glomerata in vitro cultures

The treatments were constituted of the two abovementioned accessions, infected or not infected with nematode. After 15 days, it was performed by adding an aqueous solution containing 10,000 Meloidogyne javanica eggs in one of the split roots of each plant. After 15 days of the inoculation, the substrate was enriched with the liquid fertilizer "Ouro Verde " in the following proportions : 25 % of total N, 15 % P_2O_5, 10 %

K_2O , 0.7 % B and 0.7 % Zn). Elapsed 90 days after soil infestation, it was determined the content of the (20E) in all plant organs, and the shoots were collected for metabolomics.

20-hydroxyecdysone content (20E)

The content 20Ein the shoot of Pfaffia glomerata in all treatments was determined using high-performance liquid chromatography (HPLC) following the methodology proposed by Kamada et al. (2009). The methanolic extracts were analyzed by HPLC Shimadzu (LC- 10AI model , Tokyo, Japan) equipped with a CBM -10A detector Bondesil C18 chromatographic column (4.6mm x 5.0 μm x 250 mm) , mobile phase was methanol: water (1:1) in an isocratic flow 0.7 $ml.min^{-1}$. The sample injection volume was 20 μL analyzed and wavelength 245 nm.

Pfaffia glomerata leaf metabolite sample preparation for CG-MS

Plant material was prepared for metabolite analysis according to Lisec et al. (2006) with modifications. Briefly, leaves of the plantlets were collected at the middle of the light period and frozen in liquid nitrogen, then stored at -80 ºC until sample preparation. A 10 mg sample lyophilized leaf tissue was ground to a fine powder with amortar and pestle in the presence of liquid nitrogen and then extracted with 1.5 mL of extraction buffer water: methanol:chloroform (1:2.5:1) and ribitol (0.2 mg. mL^{-1}) to correct for the loss of analytes during sample preparation or sample injection. Metabolites were extracted from the sample by incubation for 30 min at 4 °C and 950 rpm and then the supernatant (1 mL) was collected. It was added to the supernatant 750 µL of water, and then was centrifugated for 15 min, at 4°C, at 12000 rpm. Aliquot of 50 µl was collected and subsequently dried in a speed-vacuum. The residue was derivatized for 120 min at 37 °C (in 40µL of 20 mg mL^{-1} methoxyamine hydrochloride dissolved in pyridine), followed by a 30-min treatment at 37 °C with 70 µL of MSTFA [N-methyl-N-(trimethylsilyl)trifluoroacetamide]. Prior to trimethylsilylation, 20µL of a retention time standard mixture was added—3.7% (w/v) for hepatonic acid, nonanoic acid, undecanoic acid, and tridecanoic acid; 7.4% (w/v) for pentadecanic acid, nonadeanoic acid, and tricosanoic acid; 22.2% (w/v) for heptacosanoic acid55.5% (w/v) for then

triacontanoic acid dissolved in 50 mg/5 mL^{-1} tetrahydrofuran. One-microliter of each sample was injected with a split ratio of 25:1.

GC-MS analysis

The separation was performing using na Agilent 7890 A GC equipped with a 30-m MDN-35 column (Macherey-Nagel) and analytes were detected using a LecoTruTOF® HT TOFMS (Leco Corporation, St Joseph, USA; Lisex et al. 2006). Samples (1µL) were injected in splitless mode at 230ºC usign helium as carrier gas as contínuos flow of 2 ml min^{-1}. The GC oven temperature was initially maitained constant as 80ºC and the increased at a rate of 15ºC min^{-1} to 330ºC. The chromatograms were aligned using the MetAlign software (Lommen 2009). Peak identification was performing using ChromaTOF (LEGO) and a library of TMS derivatized compounds from the Max Planck Institute for Molecular Plant Biology, Germany and validated with the TagFinder software (Luedemann et al 2008). Peak intensities were corrected for variations in the response of the internal standard and the exact mass of tissue extracted.

RNA extraction, cDNA synthesis and RT-qPCR analysis

Total RNA was isolated from P glomerata leaves after 90 days of interaction with the nematodes using TRI Reagent® (Sigma-Aldrich, St. Louis, Missouri, United States) and treated with DNAse I (Thermo Scientific NanoDrop Technology, Wilmington, Dalaware, United States) to remove genomic DNA contamination. First-strand cDNA was synthesized from from 500 ng of the total RNA using the MMLV Reverse Transcriptase, (Ludwig Biotec®, Alvorada, Brazil).

Ecdysteroid 25-hydroxylase (“Phantom” - Cyp306a1) and cytochrome P450 family 307 subfamily A (“Spook” - Cyp307a1) expression levels were assessed by qRT-PCR with gene specific primers. qRT-PCR was conducted on a CFX96 Touch™ (BIO-RAD). The Pfaffia glomerata glycerol-3-phosphate dehydrogenase gene (PgGAPDH) was used as an internal reference gene with specific primers. The primers were obtained from a P. glomerata transcriptome (in preparation).

Primers sets used were as follows: GAPDH glyceraldehyde 3-phosphate dehydrogenase, forward primer (5´-GCCAGCCCTCAATGGTAAGT-3´), reverse primer (5´-CGGTGTAACCAAAATGCCC-3´), and P. glomerata CYP306A1,

ecdysteroid 25-hydroxylase [Phantom], forward primer (5´-GTCCTGGTGATGTTGGCCT-3´), reverse primer (5´-TGGGCATGGAATAGCACGTA-3´), and Cytochrome p450, Family 307, subfamily A [Spook], forward primer (5´-GCGGTACGATGAAGGTCGAT-3´), reverse primer (5´-TCAACCCTAGCCACGTTTCC-3´). PCR programs were as follows: 2 min at 50 ºC and 10 min at 90 ºC, followed by 40 cycles of 16 s at 95 ºC and 1 min at 60ºC, and 15 s at 95 ºC, 1 min at 60 ºC, 30 s at 95 ºC, and 15 s at 60 ºC. Transcript levels were determined using the $2^{-\Delta\Delta Ct}$ method (Livak and Schmittgen 2001) with three biological replicates and at least three technical replicates (reactions), being each technical replicate composed by one PCR reaction in an individual well. The data were statistically analyzed by one-way analysis of variance (ANOVA), with the means compared by Dunnet's test, with 5% significance level.

RESULTS AND DISCUSSION

Pfaffia glomerata growth with and without the presence of Meloidogyne javanica

There wasn't diferrence on Pfaffia glomerata shoot grown in greenhouse under inoculation of nematode (Table 4). Roots lenghs of accesion 43 under M. javanica interaction was decrease problably due presense of galls.

Table 4. Shoot and roots lenght of Pfaffia glomerata accessions (22 and 43) in the greenhouse under Meloidogyne javanica inoculation after 90 days of ccultivation

Shoot Length (mm)		
Interaction with Nematode	Accession	
	22	43
Control group	171.00 Aa	138.33 Ba
Infected Plant	196.33 Aa	150.00 Ba
Root Lenght (mm)		
Interaction with Nematode	Accession	
	22	43
Control group	31.33 Aa	42.67 Aa
Infected Plant	30.00 Aa	29.33 Ab

Means followed by the uppercase capital letters horizontally and, lowecase vertically dor not statistically different among them as assessed by the Scott and Knott's test at the 5% probability level

20E content in P. glomerata was increased with presence of M. javanica

Accessions 22 and 43 had their 20E content increased under nematode inoculation. The increase of 20E content may be related to the chemical response of the plant to the nematode attack (Carneiro et al. 2007), because this compound is induced by insects and nematodes (Soriano et al. 2004). In spinach, accumulation of ecdysteroids was induced in roots by insects (Schmelz et al. 1999) or by mechanical damage (Schmelz et al. 1998).

Table 5. 20-hydroxyecdysone content (ppm) in different organs of Pfaffia glomerata (leaf, stem, root and flower) grown in a greenhouse under stress inoculation of the nematode M. javanica and control group at 90 days of cultivation

Leaf		
Interaction with Nematode	Accession	
	22	43
Control group	18.27 Bb	29.13 Ab
Infected Plant	27.64 Ba	45.18 Aa
Stem		
Interaction with Nematode	Accession	
	22	43
Control group	20.24 Aa	11.94 Ba
Infected Plant	3.24 Bb	11.42 Aa
Root		
Interaction with Nematode	Accession	
	22	43
Control group	20.80 Aa	20.53 Aa
Infected Plant	23.99 Aa	19.19 Ab
Flower		
Interaction with Nematode	Accession	
	22	43
Control group	33.05 Bb	37.21 Aa
Infected Plant	38.56 Aa	33.41 Bb

Means followed by the uppercase capital letters horizontally and, lowecase vertically dor not statistically different among them as assessed by the Scott and Knott's test at the 5% probability level

Metabolomics of Pfaffia glomerata with and without Meloidogyne shows specific differences between accessions

For metabolomic analysis, 5 shoots of control plants and plants inoculated were collected. Metabolite analysis is heatmap in Figure 3, demonstrating that accessions 22 and 43 of P. glomerata have dichotomous characteristics, which helps us to verify the intensity and pattern of response in primary metabolism that go beyond the specific differences of organisms when evaluated under stress induced by inoculation with the root-knot nematode Meloidogyne javanica.

The primary metabolic profile analysis proved the difference between the accessions 22 and 43. These accessions showed different patterns of accumulation of secondary 20E compound since they accumulate this metabolite in different organs. The Ac 43 is considered a good accumulator of 20E on the leaves, whereas Ac 22 accumulates 20E mainly in roots. These accessions were previously selected by presenting divergent 20E production levels. According to Kamada (2006), Ac 22 averaged 0.749 % 20E, while the Ac 43 showed 0.346 % in the dry root mass. Iarema (2008) found for accessions 22 and 43, 1.58 % and 0.86 % of 20E.

The presence of M. javanica reduce many central metabolites of the Ac 43, mainly organic acids from the citrate cycle, and enhanced the amino acids turnover. Antagonistic behavior was found in Ac 22. These metabolite profiles reflect remarkable changes in nitrogen assimilation in the Ac 43 of P. glomerata. Citrate accumulation could be more probably related to TCA increase, which would be consistent with an increase in metabolic activity present in galls. In cytosol, citrate can be cleaved in acetyl-CoA which is the main precursor of fatty acid and sterol biosynthesis (Suh et al. 2001), and it may be suggested that in nematode-plant interactions, citrate and malate are carbon sources for nematode nutrition (Udvardi and Day 1997). Moreover, unlike plant and other vertebrate animals, nematodes do not have the de novo sterol biosynthetic pathway (Chitwood and Lusby 1991) the sterols necessary for nematode growth and development should be supplied by the plant cells. These factors may indicate the reason for nematode-plant interaction influence the content of Pfaffia glomerata 20E (phytosteroids).

This specific plant metabolic phenotype coincides with explanation of the changes in the plant metabolites is an interaction of M. javanica and nitrogen metabolism in the Pfaffia glomerata. Organic acid sugar turnover is enhanced and directed into nitrogen assimilation and amino acid turnover like show Scherling et al. (2009).

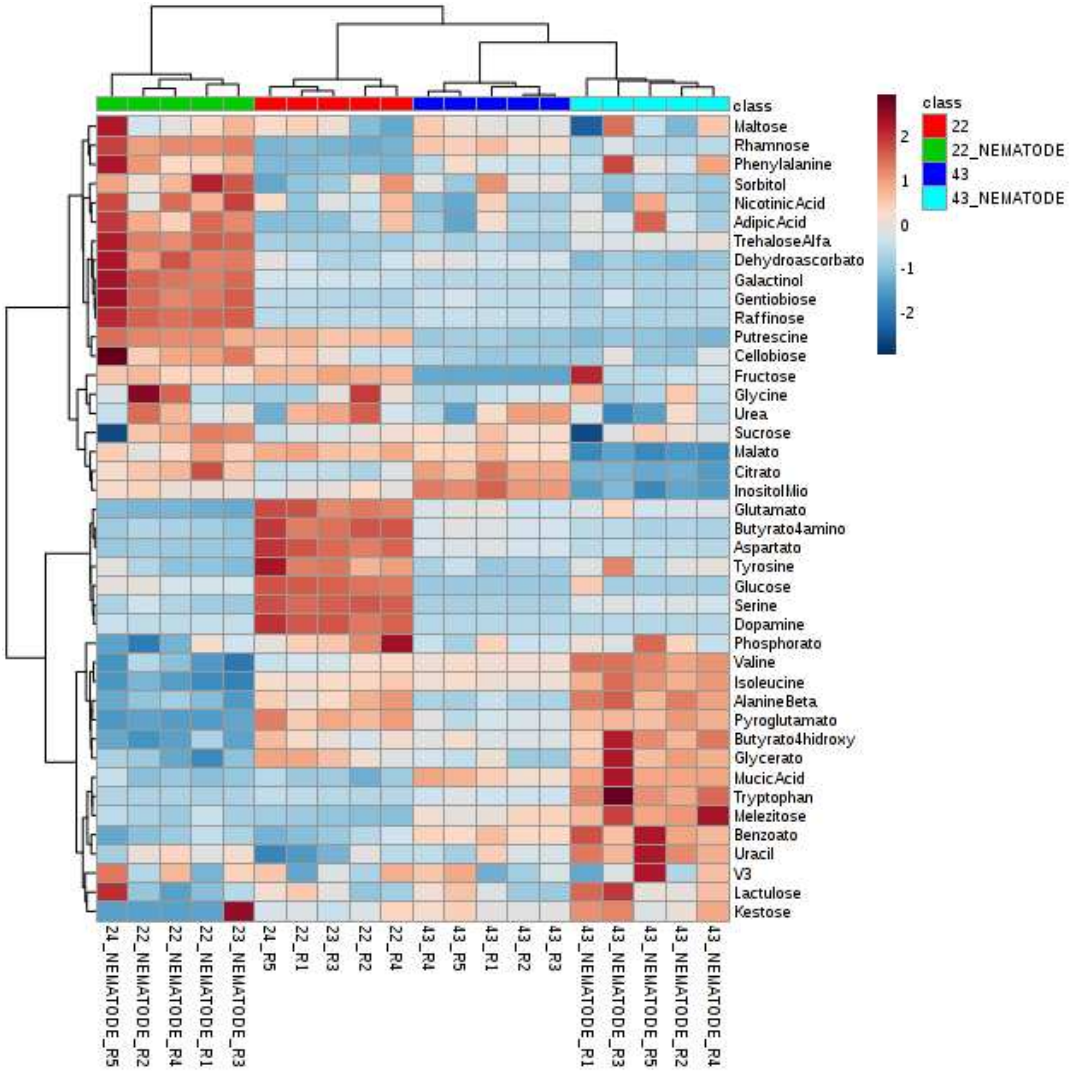

Figure 3. Heat map and hierachical cluster analysis of 41 metabolites recovered from leaves of accessions of P. glomerata (22 and 43) infected (NEMATODE) or not infected by Meloidogyne javanica. In the heat map, red color indicates high, and blue low metabolites concentration values.

Accession 22 decreases aminoacids important for nematode nitrogen nutrition

The primary metabolic profile of the accessions 22 and 43 showed diferences on accumulation pattern and reduced metabolites in response to inoculation of nematodes. The amino acids content in Ac 22 decreased when compared to the uninoculated control, in particular valine, isoleucine, serine, aspartic acid, glutamic acid, tyrosine (Table 10 on appendix). The changes of amino acids, particularly isoleucine and valine, not synthesized by the nematodes, is probably relevant for nematode nitrogen nutrition (Baldacci-Cresp et al. 2015). On the other hand, accession 43 leaves accumulate only tryptophan under nematoide accumalation and there is no changes in ohter aminoacids.

Accession 22 accumulated sugars in response to osmotic and water stress related to maturation of nematode

As the sugars (Table 10 on appendix), it was observed increase of rhamnose, frucotse, sucrose, trehalose, gentiobiose, galactinol, raffinose levels in accession 22 of Pfaffia glomerata under interaction with nematode, whilst decrease in accession 43, except trehalose, gentiobiose, galactinol and raffinose. Sugars like myo-inosiltol decrease on accession 43 while melezitose increases the contente under interaction. Only sugar that decrease on acession 22 under infection was glucose.The accumulated sugars are indicators of stress, often interfere in response to adjustments and reprogramming, as well as the accumulation of sugar alcohol galactinol. Sucrose is a well-characterized osmoregulatory compound, which accumulation is observed in many plants in response to osmotic and water stress (Gavaghan et al. 2011), and the maturation of nematode and their nematode-plant interaction is related to water stress (Baldacci-Cresp et al. 2015).

The nematodes are able to mediate the expression of genes controlling the synthesis of various metabolites. The genes, like sucrose transporters, starch synthases, myo-inositol oxygenases, myo-inositol phosphate oxygenase, sucrose UDP-glucose dehydrogenase (UGD) and ascorbic acid metabolism related to high metabolic activity, were preferentially upregulated (Hofmann and Grundler 2007; Hofmann et al. 2007; Hofmann et al. 2008; Afzal et al. 2009; Hofmann et al. 2009a; Hofmann et al. 2009b;

Siddique et al. 2009; Szakasits et al. 2009; Barcala et al. 2010; Hofmann et al. 2010; Siddique et al. 2012).

It is noteworthy that the contrasting characteristics between the accessions may be due to differential sensitivity of each accession to attack by nematodes occurring distinct responsiveness in metabolic rate more intense. Cruz (2011) noted that the observed quantities of eggs and galls on both accessions suggest tolerance to nematode of two accessions, as both accessions (22 and 43) showed large amount of eggs housed along its roots.

The increase of trehalose in Ac 22 was related to plant-microbe interaction process

In this experiment, α-trehalose accumulated in P. glomerata Ac 22 infected by netamote (Table 10 on appendix). Hofmann et al. (2010) used metabolomic tools to evaluate the systemic local effects of Heterodera schachtii infection in Arabidopsis roots. Trehalose was involved in the regulation of metabolic changes occurring during the plant–microbe interaction process (Baldacci-Cresp et al. 2015. Trehalo showed significant importance as demonstrated on figure 4.

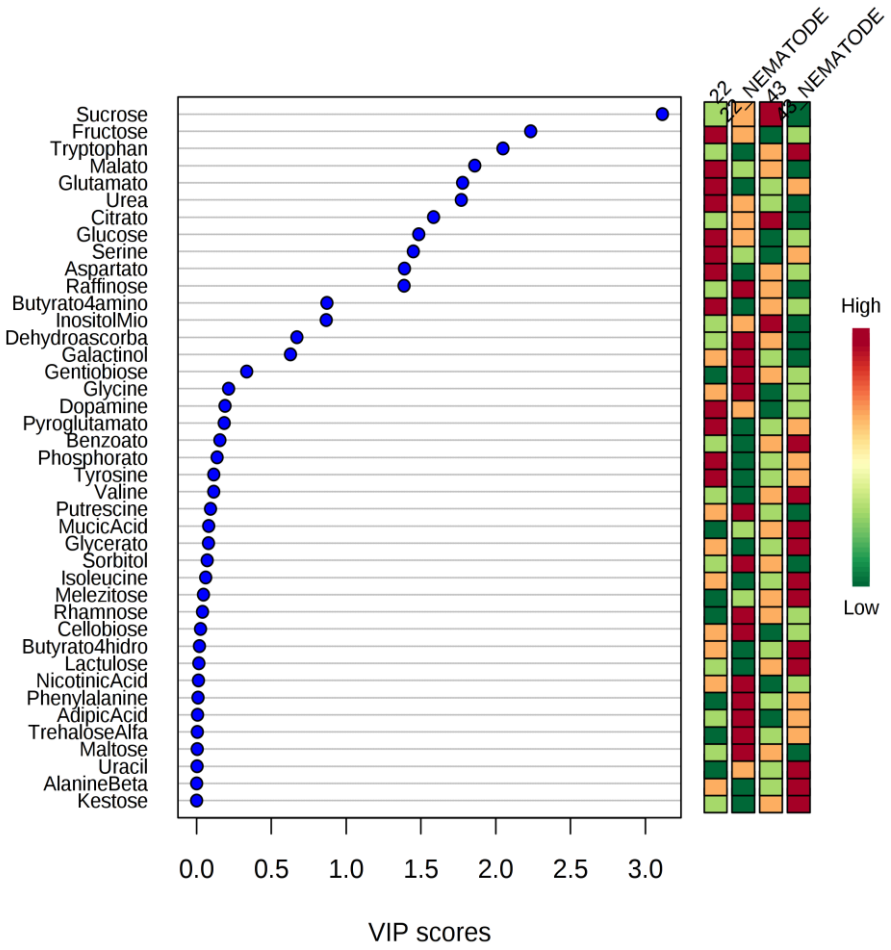

Figure 4. Score Plot of Partial Least Squeres-Discriminant Analysis (PLS-DA) of 41 compounds from leaves of accessions of P. glomerata (22 and 43) infected or not infected by Meloidogyne javanica. In the plot, red color indicates high, and green low importance

Expression of genes related to 20-hydroxyecdysone synthesis in Pfaffia glomerata is influenced by the interaction with nematodes

Phantom and Spook genes were downregulated in Ac 22 of Pfaffia glomerata infected by nematode, with nearly a 5 and 2.5-fold lower expression decrease, respectively (Fig. 5a), while that genes were upregulated in Ac 43 of P. glomerata infected by nematode (Fig. 5b).

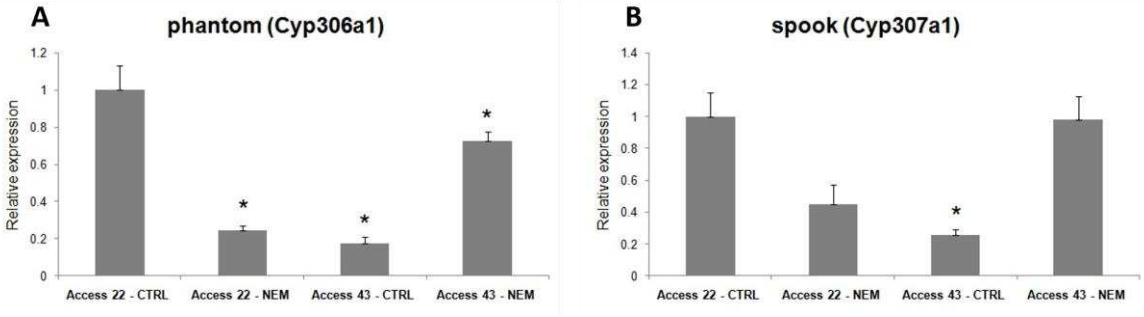

Figure 5. Real-time reverse transcription-polymerase chain reaction (RT-qPCR) for Pfaffia glomerata genes – **a)** Ecdysteroid 25-hydroxylase ("phantom" - Cyp306a1) and **b)** cytochrome P450 family 307 subfamily A ("spook" - Cyp307a1). Relative gene expression of two accessions (22 and 43) at two condition: infected by Meloidogyne javanica and control (not infected). Gene expression relative to alcohol dehydrogenase. Data presented as mean ± standard deviation, *$p<0.05$.

We monitored the expression of the Halloween genes in Pfaffia glomerata, and a summary of these pathways in insects, with the main metabolites and enzymes are shown in Figure 6. The increase of 20E in P. glomerata accessions when infected by nematode follows the increase/decrease of Spook and Phantom genes, respectively. Moreover, it has been shown that ecdysteroid accumulation in some plants like spinach can be induced by mechanical or insect damage to roots (Schmelz et al. 2002). Problably in Ac 22, the Spook and Phanton genes are inhibited by 20E contents, which it could be a feedback regulation for the 20E balance in plant tissue, as suggested by Canals et al. (2005) and Bakrim et al. (2008).

Phantom encodes 25-hydroxilase in insects (Warren et al. 2004) and Spook gene is essential for the terminal hydroxylation steps in ecdysteroid biosynthesis in the protoracid gland in insects (Namiki et al. 2005). Also, the Halloween genes modulate cytocrome P450 enzymes in insects, and that be located in the microsomes and/or

mitochondria (Petrick et al. 2003). So, it has been reported that microsomes from spinach catalyse the hydroxylation of Ecdysone to 20E as well (Grebenok and Galbaraith 1996), contrasting with its mitochondrial location in insects.

In this context, the presence of genes “Spook” and “Phantom”, analogous to insects, on 20-hydroxiecdysone biosynthesis modulation in P.glomerata can be suggested, which until now was unknown in plants. Fujimoto et al. (2015) suggests in their work, an intermediary immediately after cholesterol in the biosynthesis of 20-hydroxyecysteine in Ajuga roots. This pathway would be different from that presented by the insects that have 7dC (Fig. 6) as immediate intermediary after cholesterol. Our work infers the metabolic pathway to be similar to that of insects due to the presence of the spook gene in P. glomerata acting on intermediary 7dC. We suggest that the infection of nematode causes damage-induced accumulation of phytoecdysteroids in P. glomerata, problably by root response involving jasmonate that modulate P450 citocromes similar to Haloween genes, as demonstrated in Khaksar et al. (2017). Gomes et al (2010) suggest something similar: the increase of 20E content in P. glomerata, appears to protect the from plant from M. javanica and is described as a pos-invasion mechanism.

CONCLUSION

Our results show that Meloidogeny javanica induce a regulation of many metabolites of accessions 43 and 22 of Pfaffia glomerata. The content of 20E in P. glomerata increase with nematode infection problably because root damage-induced was modulated by the Phantom and Spook genes. Interestinlgy, both genes studied were expressed in P. glomerata. This first work on the expression of these genes in plants. They have influencerelation with the content of 20E in both accessions of P. glomerata, being downregulated by the content of 20E in the Ac 22. The metabolomic was in this work a critical tool for establishments of differences in both accessions and important compounds involved in nematode-plant interaction.

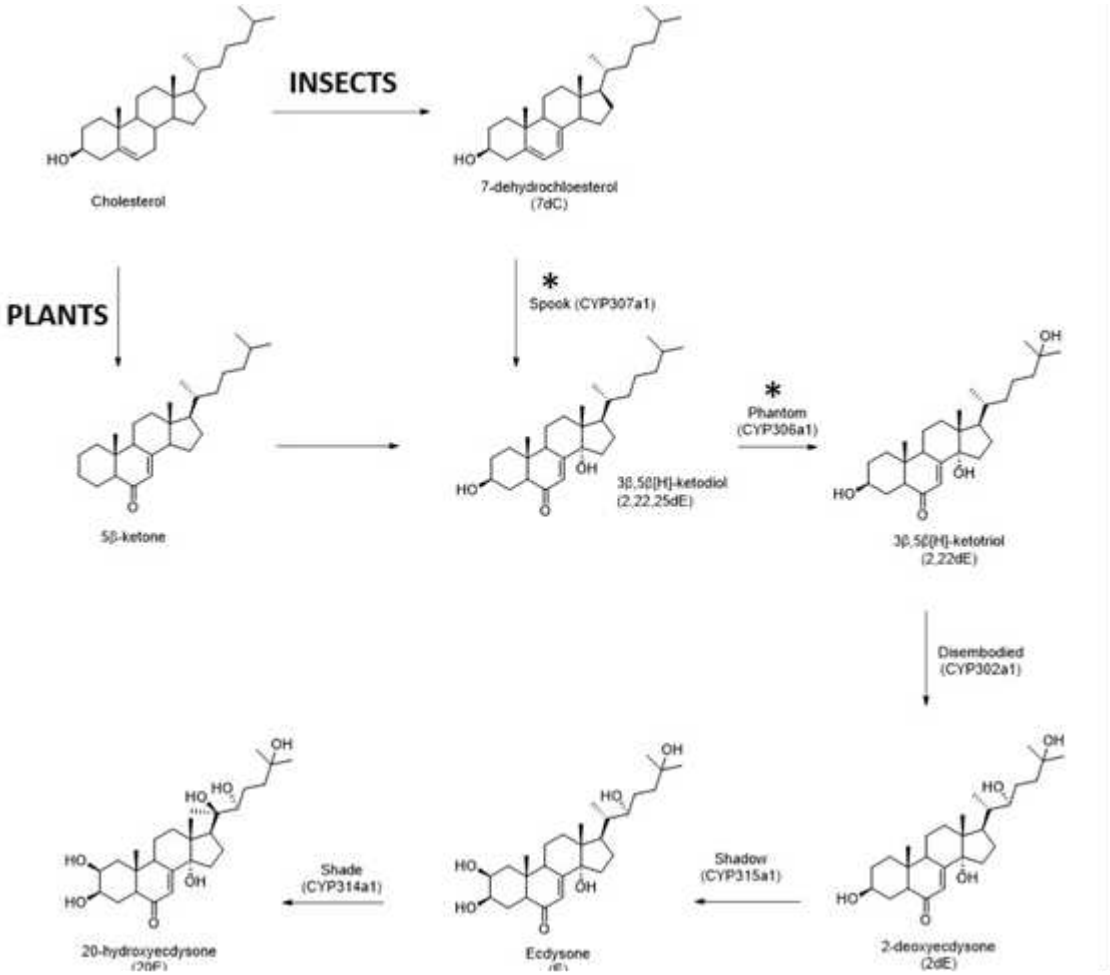

Figure 6. Summarized biosynthetic pathway of ecdysteroid biosynthesis in insects and plants. The following genes (Halloween genes) and metabolites are shown cholesterol, 5-β-ketone, 7-dehydrochloesterol (7dC), spooky (CYP307a1), 3β,5β[H]-ketodiol (2,22,25dE), phantom (CYP306a1), 3β,5β[H]-ketotriol (2,22dE), disembodied (CYP302a1), 2-deoxyecdysone (2dE), shadow (CYP315a1), ecdysone(E), shade (CYP314a1), 20-hydroxyecdysone (20E). Enzymes marked with asterisk for expression analysis. Modified from Ekert et al. (2016) and Fujimoto et al. (2015).

FUTURE TRENDS

Understanding the biosynthtic pathway(s) of ecdysteroids in plants is a challenge because it is still incomprehensible how plants produce the same molecules as insect molting hormones. Until now, almotst nothing has been published in this area, so our work is promising in this study when using Pfaffia glomerata that has high content of 20E. In this species 20E can be modulated by CO_2 enrichment and nematode interaction. In this way, we use of critical tools like metabolomics, ultrastructure and expression of genes on understanding of compunds involved in 20E biosynthesis,

changes in organels and gene regulation summarized in Table 1. Therefore, the findings of our work open a way of researches on gene expression, genetic transformation, proteomics, cell suspensions tha will allow a better understanding of 20-hydroxyecdysone biosynthesis.

Table 6. Summary of the critical components analyzed in the two chapters: 20E content, metabolomics, ultrastructure and gene expression. In the first chapter were analyzed two accessions of Pfaffia glomerata (22 and 43) on two supporting material for explant (ágar and Florialite®) under two concentrations of CO_2 (360 and 1000 µL L^{-1}). In the second chapter, two accessions of Pfaffia glomerata (22 and 43) infected or not by Meloydogene javanica were analyzed.

		CO_2-enrichment								**Nematode interaction**			
Supporting material		**Ágar**				**Florialite®**							
CO_2 concentration		360 µL L^{-1}		1000 µL L^{-1}		360 µL L^{-1}		1000 µL L^{-1}		Infected		Not infected	
Accession of Pfaffia glomerata		22	43	22	43	22	43	22	43	22	43	22	43
Secondary metabolism	20E content	-	-	-	-	-	-	+	+	+	+	-	-
Primary Metabolism	Amino acids	+	+	-	-	+	+	_	_	-	+	+	-
	Sugar	_	_	+	+	_	_	+	+	-	+	+	-
	Organic Acid	_	_	+	+	_	_	+	+	+	-	-	-
	Polyamines	+	+	-	-	+	_	+	_	+	-	+	-
	Urea	+	+	+	_	+	_	_	_	+	-	+	+
	Aromatic amines	+	-	+	-	+	-	-	-	-	+	+	-
	Shikimate	+	+	-	+	-	-	-	+	**NA**	**NA**	**NA**	**NA**
	Myo-inositol	-	-	-	+	-	-	-	+	**NA**	**NA**	**NA**	**NA**
	TCA cycle	-	-	+	-	-	+	-	+	+	-	-	+
	Trehalose	**NA**	**NA**	**NA**	**NA**	**NA**	**NA**	**NA**	**NA**	+	-	-	-
Ultrastructure	Chroloplast maturation	-	-	-	-	-	-	+	+	**NA**	**NA**	**NA**	**NA**

Gene expression	Halloween genes	**NA**	**NA**	**NA**	**NA**	**NA**	**NA**	**NA**	**NA**	**+**	**_**	**_**	**+**

*NA = Not avaliated

+ = Content was increased

_ = Conted was decreased

REFERENCES

Afzal AJ, Natarajan A, Saini N, Iqbal MJ, Geisler M, El Shemy HA, Mungur R, Willmitzer L, Lightfoot DA (2009) The Nematode Resistance Allele at the rhg1 Locus Alters the Proteome and Primary Metabolism of Soybean Roots. **Plant Physiol**, 151: 1264–1280.

Alekseeva LI (2004) Ecdysone 20-Monooxygenase Activity of Cytochrome P450 in Ajuga reptans L. Plants and Cell Culture**. Appl Biochem Microbiol**, 40: 135–139.

Alves RBN, Beroni BW, Vieira RF, França SC, Ming LC, Pereira (2010) Inflûencia de diferentes meios de cultura sobre o crescimento de Pfaffia glomerata (Spreng.) Pedersen (Amaranthaceae) para conservação in vitro. **Rev Bras Plant Med,** 12:510-515.

Bakrim A, Maria A, Sayah F, Lafont R, Takvorian N (2008) Biosynthesis and regulation of phytoecdysteroids in spinach (Spinacia oleraceae L.) **Plant Physiol Biochem,** 46: 844-854.

Baldacci-Cresp F, Maucort M, Deborde C, Pierre O, Moing A, Brouquisse M, Favery B, Frendo P (2015) Maturation of nematode-induced galls in Medicago truncatula is related to water status and primary metabolism modifications. **Plant Sci**, 232:77-85.

Barcala M, Garcia A, Cabrera J, Casson S, Lindsey K, Favery B, Garcia-Casado G, Solano R, Fenoll C, Escobar C (2010) Early transcriptomic events in microdissected Arabidopsis nematodeinduced giant cells. **Plant J**, 61: 698–712

Boneti JIS, Ferraz S (1981) Modificação do método de Hussey & Barker para extração de ovos de Meloidogyne exigua de raízes de cafeeiro. **Fitopatol Bra**s, 6:553.

Buszczak M, Segraves WA (2000) Insect Metamorphosis: Out with the old in with the new. **Curr Biol,** 10: 830-833.

Canals D, Irurre-Santilari J, Casas J (2005) The first cytochrome P450 in ferns. Evidence for its involvement in phytoecdysteroid biosynthesis in Polypodium vulgare. **FEBS Journal**, 272: 4817-4825.

Carneiro RMDG, Mesquita LFG, Cirotto PAS, Pereira SIV, Pereira PS, Silva DB, Vieira RF (2007) Detecção de Meloidogyne spp. em Pfaffia spp. no Distrito Federal e patogenicidade de M. javanica a Pfaffia glomerata e P. paniculata. **Nematologia Bras**, 30:159-163.

Chitwood DJ, Lusby WR (1991) Metabolism of plant sterols by nematodes. **Lipids,** 26:619–627

Cruz ACF (2011) **Interações entre acessos de fáfia [Pfaffia glomerata (Spreng.) Pedersen] com nematoides (Meloidogyne incognita e M. javanica): aspectos fitoquímicos e estruturais**. Tese (Doutorado em Botânica). Universidade Federal de Viçosa.

Decraemer W, Hunt DJ (2006) Structure and classification. In: Perry RN and Moens M (eds.) **Plant Nematol**, Oxfordshire, 4 p.

Desbrosser GG, Kopka J, Udvardi MK (2005) Lotus japonicas metabolic profiling. Development of gas chromatography-mass spectrometry resources for the study of plant-microbe interactions. **Plant Physiol**, 137:1302-1318.

Dinan L, Harmatha J, Volodin V, Lafont R (2009) Phytoecdysteroids: Diversity, Biosynthesis and Distribution. In: Guy S (ed) **Ecdysone: Structures and Functions**, ISBN 978-1-4020-9111-7, Springer, 43 p.

Ekert EV, Wang M, Miao YG, Brent CS, Hull JJ (2016) RNA interference-mediated knockdown of the Halloween gene Spookiest (CYP307B1) impedes adult eclosion in the western tarnished plant bug, Lygus hesperus. **Insect Mol Biol**, 25: 550-565.

Festucci-Buselli RA, Contim LAS, Barbosa LCA, Stuart JJ, Otoni WC (2008) Biosynthesis and potential functions of the ecdysteroid 20-hydroxyecdysone – a review. **Botany**, 86: 978-987.

Fujinomoto Y, Maeda I, Ohyama K, Hikiba J, Kataoka H (2015) Biosynthesis of 20-hydroxyecdysone in plants:3β-hydroxy-5β-cholestan-6-one as na intermediate immediately after cholesterol in Ajuga hairy roots. **Phytochemistry,** 111:59-64.

Gavaghan CL, Li JV, Hadfield ST, Hole S, Nicholson JK, Wilson ID, Howe PW, Stanley PD, Holmes E (2011) Application of NMR-based metabolomics to the investigation of salt stress in maize (Zea mays). **Phytochem Anal**, 22:214–224.

Gomes et al. (2010) Concentration of *β*-ecydisone (20E) in susceptible and resistant accessions of Pfaffia glomerata infected with Meloidogyne incognita and histological characterisation of resistance.**Nematology**, 12: 701 – 709.

Grebenok RJ, Galbraith DW, Benveniste I, Feyereisen R (1996) Ecdysone 20-monooxygenase, a cytochrome p450 from spinach, Spinacia oleraceae. **Phytochemistry,** 42: 927-933.

Hofmann J, Wieczorek K, Blochl A, Grundler FMW (2007) Sucrose supply to nematode-induced syncytia depends on the apoplasmic and symplasmic pathways. **J Exp Bot**, 58: 1591–1601.

Hofmann J, Szakasits D, Blochl A, Sobczak M, Daxbock-Horvath S, Golinowski W, Bohlmann H, Grundler FMW (2008) Starch serves as carbohydrate storage in nematode-induced syncytia. **Plant Physiol**, 146: 228–235.

Hofmann J, El Ashry Ael N, Anwar S, Erban A, Kopka J, Grundler F (2010) Metabolic profiling reveals local and systemic responses of host plants to nematode parasitism. **Plant J**, 62: 1058–1071.

Hofmann J, Hess PH, Szakasits D, Blochl A, Wieczorek K, Daxbock-Horvath S, Bohlmann H, van Bel AJE, Grundler FMW (2009a) Diversity and activity of sugar transporters in nematode-induced root syncytia. **J Exp Bot**, 60: 3085–3095.

Hofmann J, Kolev P, Kolev N, Daxbock-Horvath S, Grundler FMW (2009b) The Arabidopsis thaliana Sucrose Transporter Gene AtSUC4 is Expressed in Meloidogyne incognita-induced Root Galls. **J Phytopathol,** 157: 256–261.

Iarema L (2008) **Enxertia e propagação in vitro de fáfia [Pfaffia glomerata (Spreng.) Pedersen]**. Tese (Doutorado em Botânica) Universidade Federal de Viçosa.

Jones MGK, Payne HL (1978). Early stage of nematode-induced giant-cell formation in roots of Impatiens balsamina. **J Nematol**, 10: 70–84.

Kamada T (2006) **Avaliação da diversidade genética de populações de fáfia [**Pfaffia glomerata **(Spreng.) Pedersen] por RAPD, caracteres morfológicos e teor de β-ecdisona**. (Tese de Doutorado Genética e Melhoramento de Plantas). Universidade Federal de Viçosa.

Khaksar G, Treesubntorn C, Thiravetyan P (2017) Effect of exogenous methyl jasmonate on airborne benzene removal by Zamioculcas zamiifolia: The role of cytochrome P450 expression, salicylic acid, IAA, ROS and antioxidant activity. **Environ Exp Bot,** 138: 130–138.

Lafont R, Dauphin-Villemant C, Warren JT, Rees H (2005) Ecdysteroid chemistry and biochemistry. In: Gilbert LI, Iatrou K, Gill SS (Eds) **Comprehensive Molecular Insect Science**, Elsevier, pp,125-195.

Lafon R, Dinan L (2003) Practical uses for ecdysteroids in mammals including humans: na update. **J Insect Sci** 3:7.

Lisec J, Schauer N, Kopka J, Willmitzer L, Fernie AR (2006) Gas chromatography mass spectrometry-based metabolite profiling in plants. **Nature Protocols** 1:387-396.

Livak KJ, Schmittgen TD (2001) Analysis of relative gene expression. Data usign realtime quantitative PCR and the 2(-Delta Delta C(T)) method. **Methods**, 25:402-408.

Lommem A (2009) MetAlign: interface-driven, versatile metabolomics tools for hyphenated full-scan mass spectrometry data processing. **Anal Chem** 81:3079-3086.

Luedemann A, Strassburg K, Erban A, Kopka J (2008) Tag Finder for the quantitative analysis of gas chromatogreaphy-mass spectrometry (CG-MS)-based metabolite profiling experiments. **Bioinformatics** 24:732-737.

Murashige T, Skoog F (1962) A revised medium for rapid growth and bioassays with tobacco tissue cultures. **Physiol Plant**, 15: 473-497.

Namiki T, Niwa R, Sakudoh T, Shirai KI, Takeuchi H, kataoka H (2005) Cytochrome P450 CYP307A1/Spook: a regulator for ecdysone synthesis in insects. **Biochem Biophys Res Commun**, 337: 367-374.

Petryck A, Warren JT, Marques G, Jarcho MP, Gilbert LI, Kahler J, Parvy JP, Li Y, Dauphin-Villemant C, O'Connor MB (2003) Shade is Drophila P450 enzyme that mediates the hydroxylation of ecdysone to the steroid insec molting hormone 20-hydroxyecdysone. **Proc Natl Acad Sci USA**, 25: 13773-13778.

Scherling C, Ulrich K, Ewald D, Weckwerth W (2009) A metabolic signature of beneficial interaction of the endophyte Paenibacillus sp. Isolate and in vitro-grown poplar plants revealed by metabolomics. **Mol Plant Microbe Interact,** 22:1032-1037.

Schmelz EA, Grebenok RJ, Galbraith DW, Bowers, WS (1998) Damage-induced accumulation of phytoecdysteroids in spinach: a rapid root response involving the octadecanoic acid pathway. **J Chem Ecol**, 24:339-360.

Schmelz EA, Grebenok RJ, Galbraith DW, Bowers WS (1999) Insect-induced synthesis of phytoecdysteroids in spinach, Spinacia oleracea. **J Chem Ecol**, 25:1739-1757.

Schmelz EA, Grebenok RJ, Ohnmeiss TE, Bowers WS (2002) Interactions between Spinacia oleraceae and Bradysia impatiens: a role for hytoecdysteroids. **Arch Insec Biochem Physiol**, 51:204-221.

Siddique S, Endres S, Atkins JM, Szakasits D, Wieczorek K, Hofmann J, Blaukopf C, Urwin PE, Tenhaken R, Grundler FMW, Kreil DP, Bohlmann H (2009) Myo-inositol oxygenase genes are involved in the development of syncytia induced by Heterodera schachtii in Arabidopsis roots. **New Phytol**, 184: 457–472.

Siddique S, Sobczak M, Tenhaken R, Grundler FM, Bohlmann H (2012) Cell Wall Ingrowths in Nematode Induced Syncytia Require UGD2 and UGD3. **Plos One**, 7:e41515.

Soriano IR, Riley IT, Potter MJ, Bowers WS (2004) Phytoecdysteroids: a novel defense against plant-parasitic nematodes. **J Chem Ecol**, 30:1885-1898.

Suh MC, Yi SY, Lee S, Sim WS, Pai HS, Choi D (2001) Pathogen-induced expression of plant ATP: citrate lyase, **FEBS Lett**, 488:211–212.

Szakasits D, Heinen P, Wieczorek K, Hofmann J, Wagner F, Kreil DP, Sykacek P, Grundler FM, Bohlmann H (2009) The transcriptome of syncytia induced by the cyst nematode Heterodera schachtii in Arabidopsis roots. **Plant J**, 57: 771–784.

Udvardi MK, Day DA (1997) Metabolite transport across symbiotic membranes of legume nodules, **Annu Rev Plant Physiol Plant Mol Biol**, 48:493–523.

Vardanega R, Santos DT, Meireles MAA (2017) Proposal for fractionating Brazilian ginseng extracts: process intensification approach. **J Food Eng**, 196:73-80.

Warren JT, Petryk A, Marqués G, Parvy JP, Shinoda T, Itoyama K, Kobayashi J, Jarcho M, Li Y, O'Connor MB, Dauhin-Villemant C, Gilbert LI (2004) Phantom encodes the 25-hydroxylase of Drosophila melanogaster and Bombyx mori: a P450 enzyme critical in ecdysone biosynthesis. **Insect Biochem Mol**, 34: 991-1010.

Webster JM (1995) The Host-Parasite Relationships of Plant-Páarasitic Nematodes. In: Dawes B (ed.). **Advances in Parasitology**. Academic Press Inc., New York, USA. pp: 1–31

Zhou J, Li J, Wang R, Sheng X, Zong S, Weng Q, Luo Y (2016) Ecdysteroid titers and expression. Of Halloween genes and ecdysteroid receptor in relation to overwintering and the long larval phase in the seabuckthorn carpenterworm, Holcocerus hippophaecolus. **Entom Exp Appl**, 160: 133-146.

GENERAL CONCLUSIONS

- Supporting material has influence on Pfaffia glomerata in vitro metabolism under development photoautotrophic system;
- Photoautotrophy optimization increases 20-hydroxyecdysone contente on Pfaffia glomerata and triggers chloroplasts maturation;
- Photoautotrophy changes photosynthesis intermediaries, stress and adjustment metabolites levels;
- Urea is a good marker of photoautotrophic potential and putrescine putrescine shows differences in the stress tolerance mechanism in accessions 22 and 43 of Pfaffia glomerata;
- Pfaffia glomerata and Meloidogeny javanica interaction changes primary and secondary metabolites levels;
- Pathosystem root-knot nematode and Pfaffia glomerata is related to compounds associated with galls development, nematoide nitrogen nutrition, P. glomerata nitrogen cycle, plant-microorganism interaction and stress environment.
- Pfaffia glomerata root damage can modulate Halloween genes ("Spook" and *"Phantom*") leading to an increase of 20-hydroxyecdysone content;
- Interaction plant-nematode upregulate "Phantom" and "Spook" in Accession 43 and downregulate in Accession 22 of Pfaffia glomerata.
- First work of Halloweeng genes expression in plants;
- Accessions 22 and 43 of Pfaffia glomerata present distinct metabolism under photoautotrophic system and in the interaction with nematodes

➢

APPENDIX

Table 7. Metabolic content ($AU.mg^{-1}$) in double interactions of acessions (22 and 43) and supporting material (Agar and Florialite®) of Pfaffia glomerata under photoautotrophic system

Accession x Supporting Material Interaction		
Glycerol		
Accession	Supporting Material	
	Agar	Florialite®
22	6.71 Aa	3.71 Ba
43	2.20 Ab	2.50 Aa
Glycine		
Accession	Supporting Material	
	Agar	Florialite®
22	12.81 Ba	37.79 Aa
43	1.58 Ab	3.08 Ab
Urea		
Accession	Supporting Material	
	Agar	Florialite®
22	17.00 Aa	12.36 Ba
43	8.08 Ab	7.11 Ab
Alanine		
Accession	Supporting Material	
	Agar	Florialite®
22	1.69 Aa	1.09 Ba
43	0.72 Ab	0.64 Ab
Serine		
Accession	Supporting Material	
	Agar	Florialite®
22	48.74 Aa	34.77 Ba
43	12.46 Ab	4.50 Ab
Threonine		
Accession	Supporting Material	
	Agar	Florialite®
22	2.15 Aa	2.32 Aa
43	1.92 Aa	0.97 Bb
Fumaric acid		
Accession	Supporting Material	
	Agar	Florialite®
22	0.63 Aa	1.01 Aa
43	0.27 Aa	1.15 Ab
Nicotinic acid		
Accession	Supporting Material	
	Agar	Florialite®

22	1.08 Aa	1.08 Aa
43	0.72 Ab	0.82 Aa
	Malic acid	
Accession	Supporting Material	
	Agar	Florialite®
22	0.93 Aa	0.80 Ab
43	0.45 Bb	1.59 Aa
	Proline	
Accession	Supporting Material	
	Agar	Florialite®
22	0.13 Aa	0.14 Aa
43	0.05 Ab	0.10 Aa
	Aspartic acid	
Accession	Supporting Material	
	Agar	Florialite®
22	17.43 Aa	19.13 Aa
43	9.96 Bb	16.41 Aa
	Methionine	
Accession	Supporting Material	
	Agar	Florialite®
22	0.78 Aa	0.42 Ba
43	0.46 Ab	0.17 Bb
	Glutamine	
Accession	Supporting Material	
	Agar	Florialite®
22	8.79 Aa	3.13 Ba
43	6.97 Aa	1.38 Ba
	Xylose	
Accession	Supporting Material	
	Agar	Florialite®
22	0.77 Aa	0.50 Aa
43	0.03 Aa	0.67 Aa
	Ribose	
Accession	Supporting Material	
	Agar	Florialite®
22	11.37 Aa	6.22 Aa
43	0.42 Aa	11.03 Aa
	Pyroglutamic acid	
Accession	Supporting Material	
	Agar	Florialite®
22	74.08 Aa	46.30 Ba
43	71.51 Aa	39.51 Ba
	Glutamic acid	
Accession	Supporting Material	
	Agar	Florialite®
22	13.34 Aa	11.77 Aa

43	6.17 Bb	11.59 Ba
Rhamnose		
Accession	Supporting Material	
	Agar	Florialite®
22	0.66 Ba	0.92 Aa
43	0.43 Aa	0.64 Ab
Putrescine		
Accession	Supporting Material	
	Agar	Florialite®
22	1.13 Ba	2.15 Aa
43	1.16 Ab	0.61 Aa
Phenylalanine		
Accession	Supporting Material	
	Agar	Florialite®
22	4.27 Aa	5.44 Aa
43	4.01 Aa	1.36 Bb
Mannopyranoside		
Accession	Supporting Material	
	Agar	Florialite®
22	0.35 Aa	0.41 Aa
43	0.26 Ab	0.31 Ab
Ornithine		
Accession	Supporting Material	
	Agar	Florialite®
22	61.48 Aa	24.49 Ba
43	44.78 Ab	8.31 Bb
Mannose		
Accession	Supporting Material	
	Agar	Florialite®
22	0.15 Aa	0.13 Aa
43	0.04 Bb	0.10 Ab
Fructose		
Accession	Supporting Material	
	Agar	Florialite®
22	11.66 Aa	10.64 Aa
43	4.02 Bb	8.62 Aa
Shikimic acid		
Accession	Supporting Material	
	Agar	Florialite®
22	0.03 Ab	0.02 Aa
43	0.05 Aa	0.02 Ba
Galactose		
Accession	Supporting Material	
	Agar	Florialite®
22	0.53 Aa	0.28 Ba
43	0.17 Ab	0.24 Aa

Sorbose		
Accession	Supporting Material	
	Agar	Florialite®
22	8.50 Aa	8.00 Aa
43	3.13 Bb	6.60 Aa
Glucose		
Accession	Supporting Material	
	Agar	Florialite®
22	20.95 Aa	15.57 Bb
43	13.59 Bb	23.25 Aa
Citric acid		
Accession	Supporting Material	
	Agar	Florialite®
22	2.29 Aa	1.42 Bb
43	0.96 Bb	2.28 Aa
Lysine		
Accession	Supporting Material	
	Agar	Florialite®
22	9.47 Aa	5.47 Ba
43	4.73 Ab	1.75 Bb
Dehydroascorbic acid		
Accession	Supporting Material	
	Agar	Florialite®
22	0.03 Aa	0.03 Aa
43	0.01 Ab	0.02 Aa
Galacturonic acid		
Accession	Supporting Material	
	Agar	Florialite®
22	0.09 Aa	0.04 Bb
43	0.07 Aa	0.08 Aa
Tyramine		
Accession	Supporting Material	
	Agar	Florialite®
22	1.54 Aa	0.79 Ba
43	0.45 Ab	0.57 Aa
Ascorbate		
Accession	Supporting Material	
	Agar	Florialite®
22	0.030 Aa	0.005 Ba
43	0.010 Ab	0.002 Aa
Myo inositol		
Accession	Supporting Material	
	Agar	Florialite®
22	6.88 Aa	4.20 Ba
43	4.59 Ab	5.74 Aa
Tyrosine		

Accession	Supporting Material	
	Agar	Florialite®
22	7.39 Aa	5.80 Aa
43	4.29 Ab	2.05 Ab
	Histidine	
Accession	Supporting Material	
	Agar	Florialite®
22	14.72 Aa	2.64 Ba
43	8.96 Ab	0.98 Ba
	Dopamine	
Accession	Supporting Material	
	Agar	Florialite®
22	0.13 Aa	0.03 Ba
43	0.05 Ab	0.05 Aa
	Tryptophan	
Accession	Supporting Material	
	Agar	Florialite®
22	9.80 Aa	4.60 Ba
43	8.56 Aa	2.76 Ba
	Sucrose	
Accession	Supporting Material	
	Agar	Florialite®
22	29.63 Aa	26.04 Ab
43	18.94 Bb	34.47 Aa
	Lactulose	
Accession	Supporting Material	
	Agar	Florialite®
22	0.13 Ba	0.22 Ab
43	0.10 Ba	0.35 Aa
	Lactilol	
Accession	Supporting Material	
	Agar	Florialite®
22	0.29 Aa	0.16 Ba
43	0.11 Ab	0.14 Aa
	Trealose	
Accession	Supporting Material	
	Agar	Florialite®
22	0.02 Aa	0.02 Aa
43	0.01 Aa	0.02 Aa
	Maltose	
Accession	Supporting Material	
	Agar	Florialite®
22	0.28 Aa	0.18 Ba
43	0.08 Bb	0.21 Aa
	Isomaltose	
Accession	Supporting Material	

	Agar	Florialite®
22	3.43 Ba	8.82 Aa
43	1.39 Ba	9.28 Aa
	Gentiobiose	
Accession	Supporting Material	
	Agar	Florialite®
22	0.21 Ba	0.39 Aa
43	0.04 Ba	0.34 Aa
	Galactinol	
Accession	Supporting Material	
	Agar	Florialite®
22	0.39 Ba	0.70 Aa
43	0.09 Bb	0.59 Aa
	Raffinose	
Accession	Supporting Material	
	Agar	Florialite®
22	0.15 Aa	0.08 Aa
43	0.02 Ab	0.07 Aa

Means followed by the uppercase capital letters horizontally and, lowecase vertically dor not statistically different among them as assessed by the Scott and Knott's test at the 5% probability level.

Table 8. Metabolic content ($AU.mg^{-1}$) in double interactions of CO_2 concentration (360 and 1000 µL L^{-1}) and acessions (22 and 43) of Pfaffia glomerata under photoautotrophic system.

CO_2 Concentration x Accession Interaction		
	Glycerol	
[CO_2] µL L^{-1}	Accession	
	22	43
360	2.43 Ab	0.69 Ab
1000	7.99 Aa	4.00 Ba
	Glycine	
[CO_2] µL L^{-1}	Accession	
	22	43
360	14.96 Ab	1.66 Ba
1000	35.64 Aa	3.00 Ba
	Urea	
[CO_2] µL L^{-1}	Accession	
	22	43
360	19,39 Aa	8.41 Ba
1000	9.97 Ab	6.79 Aa
	Alanine	
[CO_2] µL L^{-1}	Accession	
	22	43
360	1.38 Aa	0.56 Ba

1000	1.39 Aa	0.80 Ba
	Serine	
$[CO_2]$ µL L^{-1}	Accession	
	22	43
360	47.41 Aa	10.58 Ba
1000	36.09 Ab	6.38 Ba
	Threonine	
$[CO_2]$ µL L^{-1}	Accession	
	22	43
360	2.44 Aa	1.66 Ba
1000	2.05 Aa	1.24 Ba
	Fumaric acid	
$[CO_2]$ µL L^{-1}	Accession	
	22	43
360	1.16 Aa	0.27 Ba
1000	0.48 Ab	0.15 Aa
	Nicotinic acid	
$[CO_2]$ µL L^{-1}	Accession	
	22	43
360	0.87 Ab	0.66 Aa
1000	1.29 Aa	0.88 Ba
	Malic acid	
$[CO_2]$ µL L^{-1}	Accession	
	22	43
360	0.79 Aa	0.93 Aa
1000	0.94 Aa	1.11 Aa
	Proline	
$[CO_2]$ µL L^{-1}	Accession	
	22	43
360	0.16 Aa	0.08 Ba
1000	0.11 Ab	0.06 Ba
	Aspartic acid	
$[CO_2]$ µL L^{-1}	Accession	
	22	43
360	22.50 Aa	14.15 Ba
1000	14.06 Ab	12.22 Aa
	Methionine	
$[CO_2]$ µL L^{-1}	Accession	
	22	43
22	0.54 Aa	0.28 Ba
43	0.66 Aa	0.35 Ba
	Glutamine	
$[CO_2]$ µL L^{-1}	Accession	
	22	43
360	6.31 Aa	5.11 Aa
1000	5.62 Aa	3.24 Aa

Xylose		
$[CO_2]$ µL L^{-1}	Accession	
	22	43
360	0.59 Aa	0.39 Aa
1000	0.68 Aa	0.31 Aa
Ribose		
$[CO_2]$ µL L^{-1}	Accession	
	22	43
360	8.41 Aa	6.10 Aa
1000	9.18 Aa	5.35 Aa
Pyroglutamic acid		
$[CO_2]$ µL L^{-1}	Accession	
	22	43
360	64.92 Aa	57.16 Aa
1000	55.46 Aa	53.86 Aa
Glutamic acid		
$[CO_2]$ µL L^{-1}	Accession	
	22	43
360	13.39 Aa	8.31 Ba
1000	11.71 Aa	9.44 Aa
Rhamnose		
$[CO_2]$ µL L^{-1}	Accession	
	22	43
360	0.79 Aa	0.46 Ba
1000	0.79 Aa	0.61 Aa
Putrescine		
$[CO_2]$ µL L^{-1}	Accession	
	22	43
360	1.60 Aa	0.93 Ba
1000	1.70 Aa	0.84 Ba
Phenylalanine		
$[CO_2]$ µL L^{-1}	Accession	
	22	43
360	4.79 Aa	3.67 Aa
1000	4.91 Aa	1.70 Bb
Mannopyranoside		
$[CO_2]$ µL L^{-1}	Accession	
	22	43
360	0.42 Aa	0.31 Ba
1000	0.35 Aa	0.26 Ba
Ornithine		
$[CO_2]$ µL L^{-1}	Accession	
	22	43
360	40.56 Aa	30.10 Ba
1000	45.41 Aa	23.00 Ba

Mannose		
$[CO_2]$ µL L^{-1}	Accession	
	22	43
360	0.06 Ab	0.02 Bb
1000	0.23 Aa	0.12 Ba
Fructose		
$[CO_2]$ µL L^{-1}	Accession	
	22	43
360	4.60 Ab	1.89 Bb
1000	17.70 Aa	10.75 Ba
Shikimic acid		
$[CO_2]$ µL L^{-1}	Accession	
	22	43
360	0.02 Ba	0.04 Aa
1000	0.03 Aa	0.03 Aa
Galactose		
$[CO_2]$ µL L^{-1}	Accession	
	22	43
360	0.12 Ab	0.08 Ab
1000	0.69 Aa	0.33 Ba
Sorbose		
$[CO_2]$ µL L^{-1}	Accession	
	22	43
360	0.12 Ab	1.39 Ab
1000	13.37 Aa	8.33 Ba
Glucose		
$[CO_2]$ µL L^{-1}	Accession	
	22	43
360	8.46 Ab	11.70 Ab
1000	28.06 Aa	25.14 Aa
Citric acid		
$[CO_2]$ µL L^{-1}	Accession	
	22	43
360	1.76 Aa	1.60 Aa
1000	1.95 Aa	1.63 Aa
Lysine		
$[CO_2]$ µL L^{-1}	Accession	
	22	43
360	6.44 Aa	3.41 Ba
1000	8.49 Aa	3.06 Ba
Dehydroascorbic acid		
$[CO_2]$ µL L^{-1}	Accession	
	22	43
360	0.03 Aa	0.01 Aa
1000	0.03 Aa	0.02 Aa
Galacturonic acid		

$[CO_2]$ µL L^{-1}	Accession	
	22	43
360	0.08 Aa	0.09 Aa
1000	0.06 Aa	0.06 Aa
	Tyramine	
$[CO_2]$ µL L^{-1}	Accession	
	22	43
360	1.44 Aa	0.50 Ba
1000	0.90 Ab	0.52 Aa
	Ascorbate	
$[CO_2]$ µL L^{-1}	Accession	
	22	43
360	0.012 Aa	0.008 Aa
1000	0.021 Aa	0.004 Ba
	Myo inositol	
$[CO_2]$ µL L^{-1}	Accession	
	22	43
360	4.85 Aa	4.35 Aa
1000	6.23 Aa	5.98 Aa
	Tyrosine	
$[CO_2]$ µL L^{-1}	Accession	
	22	43
360	7.33 Aa	3.43 Ba
1000	5.86 Aa	2.91 Ba
	Histidine	
$[CO_2]$ µL L^{-1}	Accession	
	22	43
360	8.29 Aa	7.12 Aa
1000	9.07 Aa	2.82 Ba
	Dopamine	
$[CO_2]$ µL L^{-1}	Accession	
	22	43
360	0.09 Aa	0.08 Aa
1000	0.07 Aa	0.03 Bb
	Tryptophan	
$[CO_2]$ µL L^{-1}	Accession	
	22	43
360	8.48 Aa	8.27 Aa
1000	5.92 Aa	3.05 Ab
	Sucrose	
$[CO_2]$ µL L^{-1}	Accession	
	22	43
360	41.47 Aa	36.44 Aa
1000	14.20 Ab	16.98 Ab
	Lactulose	
$[CO_2]$ µL L^{-1}	Accession	

	22	43
360	0.16 Aa	0.22 Aa
1000	0.19 Aa	0.24 Aa
	Lactilol	
$[CO_2]$ µL L^{-1}	Accession	
	22	43
360	0.23 Aa	0.12 Ba
1000	0.23 Aa	0.12 Ba
	Trealose	
$[CO_2]$ µL L^{-1}	Accession	
	22	43
360	0.03 Aa	0.02 Aa
1000	0.02 Aa	0.02 Aa
	Maltose	
$[CO_2]$ µL L^{-1}	Accession	
	22	43
360	0.16 Ab	0.10 Ab
1000	0.30 Aa	0.19 Ba
	Isomaltose	
$[CO_2]$ µL L^{-1}	Accession	
	22	43
360	3.69 Ab	2.72 Ab
1000	8.57 Aa	7.96 Aa
	Gentiobiose	
$[CO_2]$ µL L^{-1}	Accession	
	22	43
360	0.30 Aa	0.22 Aa
1000	0.29 Aa	0.16 Aa
	Galactinol	
$[CO_2]$ µL L^{-1}	Accession	
	22	43
360	0.62 Aa	0.41 Aa
1000	0.47 Aa	0.27 Aa
	Raffinose	
$[CO_2]$ µL L^{-1}	Accession	
	22	43
360	0.16 Aa	0.06 Ba
1000	0.07 Ab	0.02 Aa

Means followed by the uppercase capital letters horizontally and, lowecase vertically dor not statistically different among them as assessed by the Scott and Knott's test at the 5% probability level.

Table 9. Metabolic content ($AU.mg^{-1}$) in double interactions of CO_2 concentration (360 and 1000 µL L^{-1}) and supporting material (Agar and Florilaite®) of Pfaffia glomerata under photoautotrophic system.

CO_2 Concentration x Supporting Material Interaction		
Glycerol		
[CO_2] µL L^{-1}	Supporting Material	
	Agar	Florialite®
360	1.50 Ab	1.62 Ab
1000	7.41 Aa	4.58 Ba
Glycine		
[CO_2] µL L^{-1}	Supporting Material	
	Agar	Florialite®
360	7.34 Aa	9.29 Ab
1000	7.06 Ba	31.59 Aa
Urea		
[CO_2] µL L^{-1}	Supporting Material	
	Agar	Florialite®
360	15.64 Aa	12.16 Aa
1000	9.45 Ab	7.32 Ab
Alanine		
[CO_2] µL L^{-1}	Supporting Material	
	Agar	Florialite®
360	1.01 Aa	0.93 Aa
1000	1.40 Aa	0.79 Ba
Serine		
[CO_2] µL L^{-1}	Supporting Material	
	Agar	Florialite®
360	34.23 Aa	23.76 Ba
1000	26.97 Aa	15.51 Ba
Threonine		
[CO_2] µL L^{-1}	Supporting Material	
	Agar	Florialite®
360	2.40 Aa	1.70 Ba
1000	1.68 Ab	1.60 Aa
Fumaric acid		
[CO_2] µL L^{-1}	Supporting Material	
	Agar	Florialite®
360	0.55 Aa	0.88 Aa
1000	0.35 Aa	0.28 Aa
Nicotinic acid		
[CO_2] µL L^{-1}	Supporting Material	
	Agar	Florialite®
360	0.84 Aa	0.69 Ab
1000	0.96 Aa	1.21 Aa
Malic acid		

$[CO_2]$ µL L^{-1}	Supporting Material	
	Agar	Florialite®
360	0.59 Ba	1.13 Aa
1000	0.79 Ba	1.27 Aa
	Proline	
$[CO_2]$ µL L^{-1}	Supporting Material	
	Agar	Florialite®
360	0.09 Ba	0.15 Aa
1000	0.09 Aa	0.09 Ab
	Aspartic acid	
$[CO_2]$ µL L^{-1}	Supporting Material	
	Agar	Florialite®
360	15.05 Ba	21.59 Aa
1000	12.33 Aa	13.95 Ab
	Methionine	
$[CO_2]$ µL L^{-1}	Supporting Material	
	Agar	Florialite®
22	0.58 Aa	0.24 Ba
43	0.66 Aa	0.35 Ba
	Glutamine	
$[CO_2]$ µL L^{-1}	Supporting Material	
	Agar	Florialite®
360	8.52 Aa	2.90 Ba
1000	7.24 Aa	1.61 Ba
	Xylose	
$[CO_2]$ µL L^{-1}	Supporting Material	
	Agar	Florialite®
360	0.62 Aa	0.35 Aa
1000	0.18 Aa	0.81 Aa
	Ribose	
$[CO_2]$ µL L^{-1}	Supporting Material	
	Agar	Florialite®
360	8.83 Aa	5.67 Aa
1000	2.96 Aa	11.56 Aa
	Pyroglutamic acid	
$[CO_2]$ µL L^{-1}	Supporting Material	
	Agar	Florialite®
360	74.84 Aa	47.24 Ba
1000	70.75 Aa	38.57 Ba
	Glutamic acid	
$[CO_2]$ µL L^{-1}	Supporting Material	
	Agar	Florialite®
360	9.03 Aa	12.67 Aa
1000	10.48 Aa	10.68 Aa
	Rhamnose	
$[CO_2]$ µL L^{-1}	Supporting Material	

	Agar	Florialite®
360	0.56 Aa	0.69 Aa
1000	0.54 Ba	0.86 Aa
Putrescine		
$[CO_2]$ µL L^{-1}	Supporting Material	
	Agar	Florialite®
360	1.29 Aa	1.25 Aa
1000	1.00 Aa	1.51 Aa
Phenylalanine		
$[CO_2]$ µL L^{-1}	Supporting Material	
	Agar	Florialite®
360	6.01 Aa	2.45 Bb
1000	2.27 Bb	4.35 Aa
Mannopyranoside		
$[CO_2]$ µL L^{-1}	Supporting Material	
	Agar	Florialite®
360	0.35 Aa	0.37 Aa
1000	0.25 Bb	0.35 Aa
Ornithine		
$[CO_2]$ µL L^{-1}	Supporting Material	
	Agar	Florialite®
360	50.65 Aa	20.01 Ba
1000	55.61 Aa	12.80 Ba
Mannose		
$[CO_2]$ µL L^{-1}	Supporting Material	
	Agar	Florialite®
360	0.03 Ab	0.04 Ab
1000	0.16 Aa	0.19 Aa
Fructose		
$[CO_2]$ µL L^{-1}	Supporting Material	
	Agar	Florialite®
360	2.72 Ab	3.78 Ab
1000	12.96 Ba	15.48 Aa
Shikimic acid		
$[CO_2]$ µL L^{-1}	Supporting Material	
	Agar	Florialite®
360	0.04 Aa	0.01 Bb
1000	0.03 Ab	0.03 Aa
Galactose		
$[CO_2]$ µL L^{-1}	Supporting Material	
	Agar	Florialite®
360	0.09 Ab	0.11 Ab
1000	0.62 Aa	0.41 Ba
Sorbose		
$[CO_2]$ µL L^{-1}	Supporting Material	

	Agar	Florialite®
360	1.87 Ab	2.65 Ab
1000	9.76 Ba	11.95 Aa
	Glucose	
$[CO_2]$ µL L^{-1}	Supporting Material	
	Agar	Florialite®
360	8.72 Ab	11.43 Ab
1000	25.81 Aa	27.39 Aa
	Citric acid	
$[CO_2]$ µL L^{-1}	Supporting Material	
	Agar	Florialite®
360	1.40 Aa	1.96 Aa
1000	1.85 Aa	1.73 Aa
	Lysine	
$[CO_2]$ µL L^{-1}	Supporting Material	
	Agar	Florialite®
360	6.86 Aa	3.00 Ba
1000	7.34 Aa	4.21 Ba
	Dehydroascorbic acid	
$[CO_2]$ µL L^{-1}	Supporting Material	
	Agar	Florialite®
360	0.03 Aa	0.02 Aa
1000	0.01 Ba	0.04 Aa
	Galacturonic acid	
$[CO_2]$ µL L^{-1}	Supporting Material	
	Agar	Florialite®
360	0.10 Aa	0.07 Ba
1000	0.07 Ab	0.05 Aa
	Tyramine	
$[CO_2]$ µL L^{-1}	Supporting Material	
	Agar	Florialite®
360	1.12 Aa	0.82 Aa
1000	0.87 Aa	0.55 Aa
	Ascorbate	
$[CO_2]$ µL L^{-1}	Supporting Material	
	Agar	Florialite®
360	0.017 Aa	0.004 Ba
1000	0.022 Aa	0.003 Ba
	Myo inositol	
$[CO_2]$ µL L^{-1}	Supporting Material	
	Agar	Florialite®
360	5.00 Aa	4.20 Aa
1000	6.47 Aa	5.74 Aa
	Tyrosine	
$[CO_2]$ µL L^{-1}	Supporting Material	
	Agar	Florialite®

360	6.70 A	4.06 B
1000	4.99 A	3.79 A
	Histidine	
$[CO_2]$ µL L^{-1}	Supporting Material	
	Agar	Florialite®
360	13.13 Aa	2.28 Ba
1000	10.55 Aa	1.33 Ba
	Dopamine	
$[CO_2]$ µL L^{-1}	Supporting Material	
	Agar	Florialite®
360	0.11 Aa	0.06 Ba
1000	0.08 Aa	0.02 Ba
	Tryptophan	
$[CO_2]$ µL L^{-1}	Supporting Material	
	Agar	Florialite®
360	13.47 Aa	3.29 Ba
1000	4.90 Ab	4.07 Aa
	Sucrose	
$[CO_2]$ µL L^{-1}	Supporting Material	
	Agar	Florialite®
360	35.92 Aa	41.99 Aa
1000	12.66 Ab	18.52 Ab
	Lactulose	
$[CO_2]$ µL L^{-1}	Supporting Material	
	Agar	Florialite®
360	0.13 Ba	0.24 Ab
1000	0.09 Ba	0.34 A
	Lactilol	
$[CO_2]$ µL L^{-1}	Supporting Material	
	Agar	Florialite®
360	0.20 Aa	0.14 Aa
1000	0.20 Aa	0.16 Aa
	Trealose	
$[CO_2]$ µL L^{-1}	Supporting Material	
	Agar	Florialite®
360	0.02 Aa	0.02 Aa
1000	0.02 Aa	0.02 Aa
	Maltose	
$[CO_2]$ µL L^{-1}	Supporting Material	
	Agar	Florialite®
360	0.13 Ab	0.13 Ab
1000	0.24 Aa	0.25 Aa
	Isomaltose	
$[CO_2]$ µL L^{-1}	Supporting Material	
	Agar	Florialite®
360	2.54 Aa	3.87 Ab

1000	2.29 Ba	14.24 Aa
	Gentiobiose	
$[CO_2]$ µL L^{-1}	Supporting Material	
	Agar	Florialite®
360	0.18 Aa	0.34 Aa
1000	0.07 Ba	0.39 Aa
	Galactinol	
$[CO_2]$ µL L^{-1}	Supporting Material	
	Agar	Florialite®
360	0.42 Aa	0.61 Aa
1000	0.07 Bb	0.67 Aa
	Raffinose	
$[CO_2]$ µL L^{-1}	Supporting Material	
	Agar	Florialite®
360	0.12 Aa	0.09 Aa
1000	0.04 Ab	0.05 Aa

Concentração de CO_2 x Material de suporte		
	Glycerol	
$[CO_2]$ µL L^{-1}	Supporting Material	
	Agar	Florialite®
360	1.50 Ab	1.62 Ab
1000	7.41 Aa	4.58 Ba
	Glycine	
$[CO_2]$ µL L^{-1}	Supporting Material	
	Agar	Florialite®
360	7.34 Aa	9.29 Ab
1000	7.06 Ba	31.59 Aa
	Urea	
$[CO_2]$ µL L^{-1}	Supporting Material	
	Agar	Florialite®
360	15.64 Aa	12.16 Aa
1000	9.45 Ab	7.32 Ab
	Alanine	
$[CO_2]$ µL L^{-1}	Supporting Material	
	Agar	Florialite®
360	1.01 Aa	0.93 Aa
1000	1.40 Aa	0.79 Ba
	Serine	
$[CO_2]$ µL L^{-1}	Supporting Material	
	Agar	Florialite®
360	34.23 Aa	23.76 Ba
1000	26.97 Aa	15.51 Ba
	Threonine	

$[CO_2]$ µL L^{-1}	Supporting Material	
	Agar	Florialite®
360	2.40 Aa	1.70 Ba
1000	1.68 Ab	1.60 Aa
Fumaric acid		
$[CO_2]$ µL L^{-1}	Supporting Material	
	Agar	Florialite®
360	0.55 Aa	0.88 Aa
1000	0.35 Aa	0.28 Aa
Nicotinic acid		
$[CO_2]$ µL L^{-1}	Supporting Material	
	Agar	Florialite®
360	0.84 Aa	0.69 Ab
1000	0.96 Aa	1.21 Aa
Malic acid		
$[CO_2]$ µL L^{-1}	Supporting Material	
	Agar	Florialite®
360	0.59 Ba	1.13 Aa
1000	0.79 Ba	1.27 Aa
Proline		
$[CO_2]$ µL L^{-1}	Supporting Material	
	Agar	Florialite®
360	0.09 Ba	0.15 Aa
1000	0.09 Aa	0.09 Ab
Aspartic acid		
$[CO_2]$ µL L^{-1}	Supporting Material	
	Agar	Florialite®
360	15.05 Ba	21.59 Aa
1000	12.33 Aa	13.95 Ab
Methionine		
$[CO_2]$ µL L^{-1}	Supporting Material	
	Agar	Florialite®
22	0.58 Aa	0.24 Ba
43	0.66 Aa	0.35 Ba
Glutamine		
$[CO_2]$ µL L^{-1}	Supporting Material	
	Agar	Florialite®
360	8.52 Aa	2.90 Ba
1000	7.24 Aa	1.61 Ba
Xylose		
$[CO_2]$ µL L^{-1}	Supporting Material	
	Agar	Florialite®
360	0.62 Aa	0.35 Aa
1000	0.18 Aa	0.81 Aa
Ribose		
$[CO_2]$ µL L^{-1}	Supporting Material	
	Agar	Florialite®

360	8.83 Aa	5.67 Aa
1000	2.96 Aa	11.56 Aa
	Pyroglutamic acid	
$[CO_2]$ µL L^{-1}	Supporting Material	
	Agar	Florialite®
360	74.84 Aa	47.24 Ba
1000	70.75 Aa	38.57 Ba
	Glutamic acid	
$[CO_2]$ µL L^{-1}	Supporting Material	
	Agar	Florialite®
360	9.03 Aa	12.67 Aa
1000	10.48 Aa	10.68 Aa
	Rhamnose	
$[CO_2]$ µL L^{-1}	Supporting Material	
	Agar	Florialite®
360	0.56 Aa	0.69 Aa
	0.54 Ba	0.86 Aa
1000		
	Putrescine	
$[CO_2]$ µL L^{-1}	Supporting Material	
	Agar	Florialite®
360	1.29 Aa	1.25 Aa
1000	1.00 Aa	1.51 Aa
	Phenylalanine	
$[CO_2]$ µL L^{-1}	Supporting Material	
	Agar	Florialite®
360	6.01 Aa	2.45 Bb
1000	2.27 Bb	4.35 Aa
	Mannopyranoside	
$[CO_2]$ µL L^{-1}	Supporting Material	
	Agar	Florialite®
360	0.35 Aa	0.37 Aa
1000	0.25 Bb	0.35 Aa
	Ornithine	
$[CO_2]$ µL L^{-1}	Supporting Material	
	Agar	Florialite®
360	50.65 Aa	20.01 Ba
1000	55.61 Aa	12.80 Ba
	Mannose	
$[CO_2]$ µL L^{-1}	Supporting Material	
	Agar	Florialite®
360	0.03 Ab	0.04 Ab
1000	0.16 Aa	0.19 Aa
	Fructose	
$[CO_2]$ µL L^{-1}	Supporting Material	
	Agar	Florialite®
360	2.72 Ab	3.78 Ab
1000	12.96 Ba	15.48 Aa

Shikimic acid		
$[CO_2]$ µL L^{-1}	Supporting Material	
	Agar	Florialite®
360	0.04 Aa	0.01 Bb
1000	0.03 Ab	0.03 Aa
Galactose		
$[CO_2]$ µL L^{-1}	Supporting Material	
	Agar	Florialite®
360	0.09 Ab	0.11 Ab
1000	0.62 Aa	0.41 Ba
Sorbose		
$[CO_2]$ µL L^{-1}	Supporting Material	
	Agar	Florialite®
360	1.87 Ab	2.65 Ab
1000	9.76 Ba	11.95 Aa
Glucose		
$[CO_2]$ µL L^{-1}	Supporting Material	
	Agar	Florialite®
360	8.72 Ab	11.43 Ab
1000	25.81 Aa	27.39 Aa
Citric acid		
$[CO_2]$ µL L^{-1}	Supporting Material	
	Agar	Florialite®
360	1.40 Aa	1.96 Aa
1000	1.85 Aa	1.73 Aa
Lysine		
$[CO_2]$ µL L^{-1}	Supporting Material	
	Agar	Florialite®
360	6.86 Aa	3.00 Ba
1000	7.34 Aa	4.21 Ba
Dehydroascorbic acid		
$[CO_2]$ µL L^{-1}	Supporting Material	
	Agar	Florialite®
360	0.03 Aa	0.02 Aa
1000	0.01 Ba	0.04 Aa
Galacturonic acid		
$[CO_2]$ µL L^{-1}	Supporting Material	
	Agar	Florialite®
360	0.10 Aa	0.07 Ba
1000	0.07 Ab	0.05 Aa
Tyramine		
$[CO_2]$ µL L^{-1}	Supporting Material	
	Agar	Florialite®
360	1.12 Aa	0.82 Aa
1000	0.87 Aa	0.55 Aa
Ascorbate		
$[CO_2]$ µL L^{-1}	Supporting Material	
	Agar	Florialite®

360	0.017 Aa	0.004 Ba
1000	0.022 Aa	0.003 Ba
	Myo inositol	
$[CO_2]$ µL L^{-1}	Supporting Material	
	Agar	Florialite®
360	5.00 Aa	4.20 Aa
1000	6.47 Aa	5.74 Aa
	Tyrosine	
$[CO_2]$ µL L^{-1}	Supporting Material	
	Agar	Florialite®
360	6.70 A	4.06 B
1000	4.99 A	3.79 A
	Histidine	
$[CO_2]$ µL L^{-1}	Supporting Material	
	Agar	Florialite®
360	13.13 Aa	2.28 Ba
1000	10.55 Aa	1.33 Ba
	Dopamine	
$[CO_2]$ µL L^{-1}	Supporting Material	
	Agar	Florialite®
360	0.11 Aa	0.06 Ba
1000	0.08 Aa	0.02 Ba
	Tryptophan	
$[CO_2]$ µL L^{-1}	Supporting Material	
	Agar	Florialite®
360	13.47 Aa	3.29 Ba
1000	4.90 Ab	4.07 Aa
	Sucrose	
$[CO_2]$ µL L^{-1}	Supporting Material	
	Agar	Florialite®
360	35.92 Aa	41.99 Aa
1000	12.66 Ab	18.52 Ab
	Lactulose	
$[CO_2]$ µL L^{-1}	Supporting Material	
	Agar	Florialite®
360	0.13 Ba	0.24 Ab
1000	0.09 Ba	0.34 A
	Lactilol	
$[CO_2]$ µL L^{-1}	Supporting Material	
	Agar	Florialite®
360	0.20 Aa	0.14 Aa
1000	0.20 Aa	0.16 Aa
	Trealose	
$[CO_2]$ µL L^{-1}	Supporting Material	
	Agar	Florialite®
360	0.02 Aa	0.02 Aa
1000	0.02 Aa	0.02 Aa
	Maltose	

$[CO_2]$ µL L^{-1}	Supporting Material	
	Agar	Florialite®
360	0.13 Ab	0.13 Ab
1000	0.24 Aa	0.25 Aa
Isomaltose		
$[CO_2]$ µL L^{-1}	Supporting Material	
	Agar	Florialite®
360	2.54 Aa	3.87 Ab
1000	2.29 Ba	14.24 Aa
Gentiobiose		
$[CO_2]$ µL L^{-1}	Supporting Material	
	Agar	Florialite®
360	0.18 Aa	0.34 Aa
1000	0.07 Ba	0.39 Aa
Galactinol		
$[CO_2]$ µL L^{-1}	Supporting Material	
	Agar	Florialite®
360	0.42 Aa	0.61 Aa
1000	0.07 Bb	0.67 Aa
Raffinose		
$[CO_2]$ µL L^{-1}	Supporting Material	
	Agar	Florialite®
360	0.12 Aa	0.09 Aa
1000	0.04 Ab	0.05 Aa

Means followed by the uppercase capital letters horizontally and, lowecase vertically dor not statistically different among them as assessed by the Scott and Knott's test at the 5% probability level.

Table 10. Metabolic content (AU.mg^{-1}) of Pfaffia glomerata leaves, accessions (22 and 43) in the greenhouse under Meloidogyne javanica inoculation after 90 days of ccultivation. (Factorial 2x2).

	Valine	
Interaction with Nematode	Accession	
	22	43
Control group	1.36 Aa	1.48 Aa
Infected Plant	0.92 Bb	1.68 Aa
Hydroxi-4-butiric acid		

Interaction with Nematode	Accession	
	22	43
Control group	0.16 Aa	0.15 Ab
Infected Plant	0.05 Bb	0.23 Aa
	Isoleucine	
Interaction with Nematode	Accession	
	22	43
Control group	0.99 Aa	0.98 Aa
Infected Plant	0.55 Bb	1.13 Aa
	Glycine	
Interaction with Nematode	Accession	
	22	43
Control group	2.94 Aa	1.66 Aa
Infected Plant	3.67 Aa	1.89 Aa
	Phosphoric acid	
Interaction with Nematode	Accession	
	22	43
Control group	9.61 Aa	8.00 Ba
Infected Plant	5.73 Bb	8.34 Aa
	Urea	
Interaction with Nematode	Accession	
	22	43
Control group	20.85 Aa	18.60 Aa
Infected Plant	20.81 Aa	13.40 Aa
	Glyceric acid	
Interaction with Nematode	Accession	
	22	43
Control group	4.29 Aa	4.02 Aa
Infected Plant	3.30 Aa	4.55 Aa

Benzoic acid

Interaction with Nematode	Accession	
	22	43
Control group	0.95 Ba	1.33 Aa
Infected Plant	0.82 Ba	1.43 Aa

Serine

Interaction with Nematode	Accession	
	22	43
Control group	10.80 Aa	2.40 Ba
Infected Plant	2.48 Ab	4.05 Aa

Nicotinic Acid

Interaction with Nematode	Accession	
	22	43
Control group	0.43 Aa	0.39 Aa
Infected Plant	0.46 Aa	0.39 Aa

Uracil

Interaction with Nematode	Accession	
	22	43
Control group	0.02 Ba	0.03 Ab
Infected Plant	0.03 Ba	0.04 Aa

B-alanine

Interaction with Nematode	Accession	
	22	43
Control group	0.012 Aa	0.008 Bb
Infected Plant	0.005 Bb	0.014 Aa

Malic acid

Interaction with Nematode	Accession	
	22	43
Control group	14.49 Aa	13.89 Aa

Infected Plant	11.68 Aa	6.14 Bb
Amino-4-Butyric acid		
Interaction with Nematode	Accession	
	22	43
Control group	6.36 Aa	2.80 Ba
Infected Plant	1.39 Ab	1.77 Aa
Aspartic acid		
Interaction with Nematode	Accession	
	22	43
Control group	9.43 Aa	3.47 Ba
Infected Plant	1.15 Ab	2.32 Aa
Pyroglutamic acid		
Interaction with Nematode	Accession	
	22	43
Control group	13.42 Aa	9.88 Ba
Infected Plant	5.62 Bb	12.51 Aa
Glutamic acid		
Interaction with Nematode	Accession	
	22	43
Control group	20.53 Aa	10.64 Ba
Infected Plant	3.40 Bb	10.58 Aa
Rhamnose		
Interaction with Nematode	Accession	
	22	43
Control group	0.91 Bb	1.92 Aa
Infected Plant	2.16 Aa	1.28 Bb
Putrescine		
Interaction with Nematode	Accession	
	22	43

Control group	0.44 Aa	0.18 Ba
Infected Plant	0.48 Aa	0.13 Ba
	Phenylalanine	
Interaction with Nematode	Accession	
	22	43
Control group	0.37 Aa	0.42 Aa
Infected Plant	0.42 Aa	0.44 Aa
	Adipic acid	
Interaction with Nematode	Accession	
	22	43
Control group	26.22 Aa	26.46 Aa
Infected Plant	30.65 Aa	27.60 Aa
	Fructose	
Interaction with Nematode	Accession	
	22	43
Control group	18.81 Aa	2.37 Bb
Infected Plant	14.85 Ab	8.90 Ba
	Sorbitol	
Interaction with Nematode	Accession	
	22	43
Control group	3.70 Aa	3.97 Aa
Infected Plant	3.84 Aa	3.42 Aa
	Citric acid	
Interaction with Nematode	Accession	
	22	43
Control group	33.06 Ba	48.28 Aa
Infected Plant	38.53 Aa	24.45 Bb
	Glucose	
Interaction with Nematode	Accession	

	22	43
Control group	7.85 Aa	0.73 Ba
Infected Plant	2.62 Ab	1.00 Ba
	Dehydroascorbic acid	
Interaction with Nematode	Accession	
	22	43
Control group	3.41 Ab	4.26 Aa
Infected Plant	8.22 Aa	1.98 Bb
	Myo-inositol	
Interaction with Nematode	Accession	
	22	43
Control group	17.33 Ba	22.94 Aa
Infected Plant	16.58 Aa	11.95 Bb
	Tyrosine	
Interaction with Nematode	Accession	
	22	43
Control group	2.15 Aa	1.30 Ba
Infected Plant	1.15 Ab	1.61 Aa
	Mucic acid	
Interaction with Nematode	Accession	
	22	43
Control group	0.39 Ba	0.62 Aa
Infected Plant	0.36 Ba	0.69 Aa
	Dopamine	
Interaction with Nematode	Accession	
	22	43
Control group	0.88 Aa	0.02 Ba
Infected Plant	0.07 Ab	0.02 Aa

Tryptophan

Interaction with Nematode	Accession	
	22	43
Control group	1.04 Aa	2.31 Ab
Infected Plant	0.47 Ba	10.26 Aa

Sucrose

Interaction with Nematode	Accession	
	22	43
Control group	110.94 Bb	136.26 Aa
Infected Plant	138.62 Aa	117.41 Bb

Lactulose

Interaction with Nematode	Accession	
	22	43
Control group	0.35 Aa	0.38 Aa
Infected Plant	0.33 Aa	0.41 Aa

Cellobiose

Interaction with Nematode	Accession	
	22	43
Control group	0.30 Aa	0.24 Aa
Infected Plant	0.40 Aa	0.25 Ba

α-trehalose

Interaction with Nematode	Accession	
	22	43
Control group	0.32 Ab	0.35 Aa
Infected Plant	0.87 Aa	0.48 Ba

Maltose

Interaction with Nematode	Accession	
	22	43
Control group	0.75 Aa	0.82 Aa

Infected Plant	0.76 Aa	0.78 Aa
	Gentiobiose	
Interaction with Nematode	Accession	
	22	43
Control group	1.22 Ab	1.74 Aa
Infected Plant	5.86 Aa	1.35 Ba
	Galactinol	
Interaction with Nematode	Accession	
	22	43
Control group	1.17 Ab	0.55 Aa
Infected Plant	6.16 Aa	0.34 Ba
	Raffinose	
Interaction with Nematode	Accession	
	22	43
Control group	1.51 Ab	2.60 Aa
Infected Plant	17.88 Aa	0.75 Ba
	Kestose	
Interaction with Nematode	Accession	
	22	43
Control group	0.002 Aa	0.003 Aa
Infected Plant	0.002 Aa	0.004 Aa
	Melezitose	
Interaction with Nematode	Accession	
	22	43
Control group	0.06 Ba	0.15 Ab
Infected Plant	0.07Ba	0.26 Aa

Means followed by the uppercase capital letters horizontally and, lowecase vertically dor not statistically different among them as assessed by the Scott and Knott's test at the 5% probability level